A Semi-Empirical Reaction Mechanism for n-Heptane Oxidation and Pyrolysis

T. J. HELD, A. J. MARCHESE and F. L. DRYER

*Department of Mechanical and Aerospace Engineering,
Princeton University, Princeton, New Jersey, 08544-5263, USA*

A new semi-empirical mechanism for n-heptane oxidation and pyrolysis has been developed and validated against several independent data sets, including new flow reactor experiments. Previous semi-empirical chemical kinetic mechanisms assumed that a generic n-alkyl radical, formed by abstraction of an H-atom from the parent fuel, thermally decomposes into a fixed ratio of methyl and propene. While such an approach has been reasonably successful in predicting premixed, laminar flame speeds, the mechanism lacks sufficient detail to quantitatively capture transient phenomena and intermediate species distributions. The new chemical kinetic mechanism retains significantly more detail, yet is sufficiently compact to be used in combined fluid-mechanical/chemical kinetic computational studies. The mechanistic approach is sufficiently general to be extended to a wide variety of large linear and branched alkane fuels.

*Keywords:* n-heptane; oxidation; pyrolysis

INTRODUCTION

Linear and branched alkanes comprise a large fraction of many transportation fuels. For many practical engineering issues, such as unburned hydrocarbon emissions, a reasonably detailed level of understanding of the oxidation and pyrolysis chemistry of these species is required. Unfortunately, these types of problems often involve coupled fluid-mechanical, diffusive and reactive effects. Although extensively detailed models for larger alkanes exist (e.g., Westbrook and Dryer, 1984; Dryer, 1991; Westbrook and Pitz, 1993; Lindstedt and Maurice, 1995), they involve far too many species for use in complex fluid-mechanical simulations. For instance, the steady-state one dimensional droplet modeling of Jackson and Avedisian (1993), and the more recent, transient droplet combustion calculations of Marchese et al. (1994; 1995) would not

have been possible with these full, detailed chemical kinetic mechanisms. These studies used Warnatz's 32-species, 96-reaction semi-empirical mechanism (1984a), which was reasonably successful in reproducing laminar premixed flame speeds of n-heptane/air flames. This mechanism also formed the basis for numerical studies of steady, counter-flow diffusion flames (Bui-Pham and Seshadri, 1991), and for the reduced mechanisms used in the asymptotic droplet combustion calculations of Card and Williams (1992; 1993).

The goal of the present work is the development of a simplified high-temperature oxidation and pyrolysis model for a prototypical alkane, n-heptane. This goal is achieved through semi-empirical selection of important reaction paths, based on the conditions of intended use for the model. The mechanism is successfully applied to flow reactor and shock tube experiments, and the calculation of premixed flame speeds.

The approach used in this study is similar to that proposed by Axelsson *et al.* (1986), and used in a simplified form by Warnatz (1984a). The Warnatz model for n-heptane oxidation assumes that the predominant route of n-heptane consumption is abstraction of a hydrogen atom by O, OH and H, thereby forming an n-heptyl radical:

$$C_7H_{16} + X \rightarrow C_7H_{15} + XH$$

$$X = (H/O/OH).$$
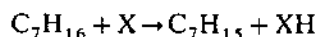
The principal empiricism in the Warnatz model is the description of the n-heptyl radical decomposition into the products of methyl and propene in fixed ratio,

$$C_7H_{15} \rightarrow CH_3 + 2C_3H_6.$$
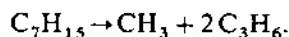
A simplified propene submechanism includes four radical addition reactions, but neglects abstraction reactions. The remainder of the mechanism involves the consumption of the C_1 and C_2 species.

Although the Warnatz mechanism is reasonably successful in modeling laminar, premixed flame speeds, it performs less successfully in other circumstances (Marchese *et al.*, 1994; 1995). The absence of initiation reactions for the fuel causes great difficulty in situations where the radical pool is not supplied by an external source, such as diffusion from a reaction zone in a premixed flame.

The chemical kinetic mechanism described in this paper contains substantial detail, yet is still compact to the extent that it may be utilized in reactive

flow computational studies. To support the development of this mechanism, a series of *n*-heptane oxidation and pyrolysis experiments were performed on a variable-pressure flow reactor. This experiment provides a means of obtaining chemical kinetic data that are relatively free from diffusive effects, at conditions similar to those in the preheat and early reaction zone of premixed and diffusion flames. Calculated results are also compared to literature stirred reactor data over a similar temperature range, using a perfectly stirred reactor approximation. For validation at higher temperatures than can be achieved in flow and stirred reactors (> 1150 K), comparisons to shock tube ignition delay data and premixed laminar flame speeds are also performed.

MODEL DEVELOPMENT

The *n*-heptane oxidation mechanism of Warnatz was initially developed for modeling steady-state, premixed laminar flame speeds. As mentioned previously, only one consumption route is postulated for the fuel — abstraction by H, O or OH, followed by thermal decomposition of the resulting heptyl radical (C_7H_{15}) to propene and the methyl radical (CH_3). In the diffusion-flame modeling of Bui-Pham and Seshadri (1991), the propene primarily reacts with OH to form acetaldehyde (CH_3HCO) and CH_3.

Three shortcomings of the Warnatz mechanism are addressed in the new mechanism. First, the absence of a thermal decomposition route for the *n*-heptane presents difficulties in the study of ignition phenomena (Marchese *et al.*, 1995). In the present calculations, these initiation reactions also consume a significant percentage of the *n*-heptane in all three types of simulations. Second, the treatment of the *n*-heptyl radical as a single species, rather than a mixture of isomers, results in a non-realistic distribution of olefinic intermediate species. The mechanism overemphasizes the importance of propene reactions, rather than those of the mixture of β-scission products measured in *n*-heptane-air diffusion flame structures (Kent and Williams, 1974) and previous flow reactor studies (Kennedy *et al.*, 1985). Finally, the C_1-C_3 submechanism, is in need of revision with current reaction paths and rate constants. The propene submechanism, in particular, lacks any abstraction routes, which are important reaction paths under combustion conditions (Westbrook and Pitz, 1984; Dagaut *et al.*, 1992).

The present modeling effort is directed toward providing a more detailed treatment of the decomposition of both the parent fuel, *n*-heptane, and the four isomeric heptyl radicals (Tab. I), while still retaining a relatively simplified view of the overall kinetics. Because each species added to a mechanism

T. J. HELD et al.

TABLE I   Isomeric n-heptyl radicals

Radical	$1\text{-}C_7H_{15}$	$2\text{-}C_7H_{15}$	$3\text{-}C_7H_{15}$	$4\text{-}C_7H_{15}$
Structure				
Type of C-H bond	Primary	Secondary	Secondary	Secondary
Number of sites	6	4	4	2
Initial β-scission products	C_2H_4 $1\text{-}C_5H_{11}$	C_3H_6 $1\text{-}C_4H_9$	$1\text{-}C_4H_8$ $1\text{-}C_6H_{12}$ $1\text{-}C_3H_7$ CH_3	$1\text{-}C_5H_{10}$ C_2H_5
Final β-scission products	$3\text{-}C_2H_4$ CH_3	C_3H_6 C_2H_4 C_2H_5	$1\text{-}C_4H_8$ $1\text{-}C_6H_{12}$ C_2H_4 CH_3 CH_3	$1\text{-}C_5H_{10}$ C_2H_5

requires solution of an additional differential equation in the kinetic system, while a new reaction only adds another term to an existing equation, a model may be extended by additional reactions without significant computational penalty. Thus, a major goal of the model development is increased site-specific detail with a relatively small number of species. Also, the $C_1 - C_3$ mechanism has been updated to a detailed kinetic mechanism developed in previous and ongoing work (Held et al., 1988; Held, 1993; Held and Dryer, 1996).

A full listing of the reaction mechanism is found in Table II. The structure of the n-heptane submechanism is similar to that of the Warnatz mechanism. The primary route of fuel consumption is still considered to be H-atom abstraction, by a somewhat larger number of radical species:

$$C_7H_{16} + X \rightarrow C_7H_{15} + XH, \qquad X = (H/O/OH/HO_2/CH_3/C_3H_5)$$
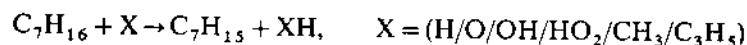
Individual rate constants are assigned to abstraction from each specific site. Rate constants are estimated using data for primary and secondary site abstraction from propane (Tsang, 1988), and adjusting the pre-exponential constant to account for the number of available H-atoms at each site (see Tab. III). In the case of n-heptane + O and OH, site-specific rate constants are available from the literature (Cohen and Westberg, 1986; Cohen, 1991).

The n-heptyl radicals are assumed, as in the Warnatz mechanism, to rapidly undergo thermal decomposition. However, the specific reaction products for each site are assumed to result from β-scission, giving a 1-olefin and a smaller alkyl radical. The product distribution from each n-heptyl isomer is listed in Table I. In the cases of 1-, 2- and 4-heptyl, only one product channel is likely. For 3-heptyl, two reaction channels are of comparable importance – the 1-hexene channel is somewhat arbitrarily assigned 20 % of the total rate, due to its slightly higher endothermicity. Alkyl radicals larger than ethyl (C_2H_5), are assumed to further decompose by β-scission, to eventually yield the final

TABLE II   Reaction mechanism

Reaction	A (cm-mol-s)	n	E_a (cal/mol)	Reference
H_2/O_2				
1. $H + O_2 = O + OH$	1.92×10^{14}	0	16439	(Pirraglia et al., 1989)
2. $O + H_2 = H + OH$	5.08×10^{04}	2.67	6290	(Sutherland et al., 1986b)
3. $H_2 + OH = H_2O + H$	2.16×10^{08}	1.51	3430	(Michael and Sutherland, 1988)
4. $O + H_2O = OH + OH$	2.97×10^{06}	2.02	13400	(Sutherland et al., 1990)
5. $H_2 + M = H + H + M$	4.58×10^{19}	-1.40	104380	(Cohen and Westberg, 1983)[b]
6. $H_2 + Ar = H + H + Ar$	5.84×10^{18}	-1.10	104380	(Cohen and Westberg, 1983)
7. $O + O + M = O_2 + M$	6.17×10^{15}	-0.50	0	(Hampson, 1980)[b]
8. $O + O + Ar = O_2 + Ar$	1.89×10^{13}	0	-1788	(Hampson, 1980)
9. $O + H + M = OH + M$	4.71×10^{18}	-1.00	0	(Tsang and Hampson, 1980)[c]
10. $H + OH + M = H_2O + M$	2.21×10^{22}	-2.00	0	(Baulch et al., 1972)[d]
$H + O_2(+M) = HO_2(+M)$	k_∞ 4.52×10^{19}	0	0	(Cobos et al., 1985)[b,e]
	k_0 6.70×10^{19}	-1.42	0	(Slack, 1977)
$H + O_2(+Ar) = HO_2(+Ar)$	k_∞ 4.52×10^{13}	0	0	(Cobos et al., 1985)
	k_0 6.17×10^{17}	-0.80	0	(Baulch et al., 1980)
	$F_{cent} = 0.5$			
11. $HO_2 + H = H_2 + O_2$	6.63×10^{13}	0	2130	(Tsang and Hampson, 1986)
12. $HO_2 + H = OH + OH$	1.69×10^{14}	0	874	(Tsang and Hampson, 1986)
13. $HO_2 + O = O_2 + OH$	1.81×10^{13}	0	-397	(Tsang and Hampson, 1986)
14. $HO_2 + OH = H_2O + O_2$	1.90×10^{16}	-1.00	0	(Kim et al., 1994)
15. $HO_2 + HO_2 = H_2O_2 + O_2$	4.20×10^{14}	0	11982	(Hippler et al., 1990)
	$+ 1.30 \times 10^{11}$	0	-1629	
16. $H_2O_2(+M) = OH + OH(+M)$	k_∞ 2.95×10^{14}	0	48430	(Brouwer et al., 1987)[b]
	k_0 1.20×10^{17}	0	45500	(Warnatz, 1984b)
	$F_{cent} = 0.5$			
$H_2O_2(+Ar) = OH + OH(+Ar)$	k_∞ 2.95×10^{14}	0	48430	(Brouwer et al., 1987)
	k_0 1.90×10^{16}	0	43000	(Brouwer et al., 1987)
	$F_{cent} = 0.5$			

TABLE II (Continued)

	Reaction	A (cm-mol-s)	n	E_a (cal/mol)	Reference
17	$H_2O_2 + H = H_2O + OH$	1.00×10^{13}	0	3590	(Warnatz, 1984b)
18	$H_2O_2 + H = HO_2 + H_2$	4.82×10^{13}	0	7950	(Tsang and Hampson, 1986)
19	$H_2O_2 + O = OH + HO_2$	9.55×10^{06}	2.00	3970	(Tsang and Hampson, 1986)
20	$H_2O_2 + OH = HO_2 + H_2O$	1.00×10^{12} $+ 5.80 \times 10^{14}$	0	0 9557	(Hippler and Troe, 1992)
CO					
21	$CO + O + M = CO_2 + M$	2.51×10^{13}	0	-4540	(Warnatz, 1984b)[f]
22	$CO + O_2 = CO_2 + O$	2.53×10^{12}	0	47700	(Tsang and Hampson, 1986)
23	$CO + OH = CO_2 + H$	1.50×10^{07}	1.30	-765	(Baulch et al., 1976)
24	$CO + HO_2 = CO_2 + OH$	6.02×10^{13}	0	23000	(Atri et al., 1977)
HCO/CH₂O					
25	$HCO + M = H + CO + M$	1.86×10^{17}	-1.00	17000	(Timonen et al., 1987b)[c]
26	$HCO + O_2 = CO + HO_2$	7.58×10^{12}	0	410	(Timonen et al., 1988)
27	$HCO + H = CO + H_2$	7.23×10^{13}	0	0	(Timonen et al., 1987a)
28	$HCO + O = CO + OH$	3.02×10^{13}	0	0	(Tsang and Hampson, 1986)
29	$HCO + O = CO_2 + H$	3.00×10^{13}	0	0	(Tsang and Hampson, 1986)
30	$HCO + OH = CO + H_2O$	3.02×10^{13}	0	0	(Tsang and Hampson, 1986)
31	$HCO + HO_2 = CO_2 + OH + H$	3.00×10^{13}	0	0	(Tsang and Hampson, 1986)
32	$HCO + CH_3 = CO + CH_4$	1.20×10^{14}	0	0	(Tsang and Hampson, 1986)
33	$HCO + HCO = CH_2O + CO$	1.80×10^{13}	0	0	(Tsang and Hampson, 1986)
34	$HCO + HCO = H_2 + CO + CO$	3.00×10^{12}	0	0	(Tsang and Hampson, 1986)
35	$CH_2O + M = HCO + H + M$	4.00×10^{23}	-1.66	91470	(Hochgreb and Dryer, 1992)
36	$CH_2O + M = CO + H_2 + M$	8.25×10^{15}	0	69540	(Roth and Just, 1984)
37	$CH_2O + H = HCO + H_2$	1.14×10^{08}	1.66	1834	(Held and Dryer, 1994)
38	$CH_2O + O = HCO + OH$	1.81×10^{13}	0	3080	(NASA, 1985)
39	$CH_2O + OH = HCO + H_2O$	4.80×10^{09}	1.18	-447	(Held and Dryer, 1994)
40	$CH_2O + O_2 = HCO + HO_2$	2.00×10^{13}	0	39000	(Baldwin et al., 1974)

	Reaction	A	n	E	Reference
41	$CH_2O + HO_2 = HCO + H_2O_2$	1.50×10^{13}	0	15200	(Hochgreb and Dryer, 1992)
42	$CH_2O + CH_3 = HCO + CH_4$	5.54×10^{03}	2.81	5862	(Tsang and Hampson, 1986)
43	$CH_2O + C_3H_5 = HCO + C_3H_6$	1.45×10^{08}	1.80	18180	(Tsang, 1991)
CH_3O					
44	$CH_3O + M = CH_2O + H + M$	8.30×10^{17}	-1.20	15500	(Page et al., 1989)
45	$CH_3O + H = CH_2O + H_2$	2.00×10^{13}	0	0	(Hoyermann et al., 1981)
46	$CH_3O + O = CH_2O + OH$	6.00×10^{12}	0	0	(Tsang and Hampson, 1986)
47	$CH_3O + OH = CH_2O + H_2O$	1.80×10^{13}	0	0	(Tsang and Hampson, 1986)
48	$CH_3O + O_2 = CH_2O + HO_2$	9.03×10^{13} $+ 2.20 \times 10^{10}$	0	11980 1748	(Wantuck et al., 1987)
49	$CH_3O + HO_2 = CH_2O + H_2O_2$	3.00×10^{11}	0	0	(Tsang and Hampson, 1986)
50	$CH_3O + CO = CH_3 + CO_2$	1.60×10^{13}	0	11800	(Lissi et al., 1973)
$CH/CH_2/CH_3$					
51	$CH + O_2 = HCO + O$	1.00×10^{13}	0	0	(Jachimowski, 1977)
52	$CH_2 + H = CH + H_2$	9.64×10^{13}	0	0	(Tsang and Hampson, 1986)
53	$CH_2 + O = CO + H + H$	1.05×10^{13}	0	0	(Tsang and Hampson, 1986)
54	$CH_2 + O = CO + H_2$	1.05×10^{13}	0	0	(Tsang and Hampson, 1986)
55	$CH_2 + O_2 = CO + OH + H$	1.13×10^{13}	0	0	(Tsang and Hampson, 1986)
56	$CH_2 + O_2 = CO + H_2O$	4.82×10^{12}	0	0	(Tsang and Hampson, 1986)
57	$CH_2 + O = CH_2O + H$	8.43×10^{13}	0	0	(Slagle et al., 1987)
58	$CH_3 + OH = CH_2 + H_2O$	1.50×10^{13}	0	5000	(Egolfopoulos et al., 1992)
59	$CH_3 + O_2 = CH_3O + O$	1.99×10^{18}	-1.57	29230	(Tsang and Hampson, 1986)
60	$CH_3 + HO_2 = CH_3O + OH$	2.00×10^{13}	0	1076	(Reid et al., 1988)
61	$CH_3 + CH_3(+M) = C_2H_6(+M)$	k_∞ 9.03×10^{16} k_0 3.18×10^{41}	-1.18 -7.03	654 2762	(Wagner and Wardlaw, 1988)
	$F_{cent} = (1 - 0.619)\exp(-T/73.2\ K) + 0.619\exp(-T/1180\ K)$				
62	$CH_3 + CH_3 = C_2H_4 + H_2$	1.00×10^{16}	0	32005	(Warnatz, 1984b)
63	$CH_3 + CH_3 = C_2H_5 + H$	8.00×10^{15}	0	26512	(Egolfopoulos et al., 1992)

TABLE II (Continued)

Reaction	A (cm-mol-s)	n	E_a (cal/mol)	Reference
CH_4				
64 $CH_4(+M) = CH_3 + H(+M)$	k_∞ 3.70×10^{15}	0	103800	(Tsang, 1989)
	k_0 7.21×10^{30}	-3.49	105900	
65 $CH_4 + H = CH_3 + H_2$	5.47×10^{07}	1.97	11210	(Schatz et al., 1984)
66 $CH_4 + O = CH_3 + OH$	6.93×10^{08}	1.56	8484	(Sutherland et al., 1986a)
67 $CH_4 + OH = CH_3 + H_2O$	5.72×10^{06}	1.96	2639	(Felder and Madronich, 1986)
68 $CH_4 + O_2 = CH_3 + HO_2$	4.00×10^{13}	0	56910	(Walker, 1975)
69 $CH_4 + HO_2 = CH_3 + H_2O_2$	1.81×10^{11}	0	18580	(Tsang and Hampson, 1986)
$C_2H/HCCO/C_2H_2$				
70 $C_2H + O = CO + CH$	1.81×10^{13}	0	0	(Tsang and Hampson, 1986)
71 $C_2H + O_2 = HCCO + O$	6.02×10^{11}	0	0	(Tsang and Hampson, 1986)
72 $C_2H + O_2 = CO + HCO$	2.41×10^{12}	0	0	(Tsang and Hampson, 1986)
73 $HCCO + H = CH_2 + CO$	3.00×10^{13}	0	0	(Warnatz, 1984b)
74 $HCCO + O = H + CO + CO$	1.20×10^{12}	0	0	(Warnatz, 1984b)
75 $HCCO + O_2 = CO + CO + OH$	1.46×10^{12}	0	2500	(Miller et al., 1982)
76 $C_2H_2 + M = C_2H + H + M$	7.46×10^{30}	-3.70	127100	(Tsang and Hampson, 1986)
77 $C_2H_2 + H = C_2H + H_2$	6.02×10^{13}	0	22250	(Tsang and Hampson, 1986)
78 $C_2H_2 + O = CH_2 + CO$	1.45×10^{06}	2.09	1560	(Michael and Wagner, 1990)
79 $C_2H_2 + O = HCCO + H$	5.78×10^{06}	2.09	1560	(Michael and Wagner, 1990)
80 $C_2H_2 + OH = C_2H + H_2O$	3.38×10^{07}	2.00	14000	(Miller and Melius, 1988)
81 $C_2H_2 + O_2 = C_2H + HO_2$	1.20×10^{13}	0	74510	(Tsang and Hampson, 1986)
82 $C_2H_2 + HO_2 = C_2H + H_2O_2$	6.03×10^{09}	0	7950	(Tsang and Hampson, 1986)

C_2H_3/C_2H_4

	Reaction	A	n	E	Reference
83	$C_2H_2 + H(+ M) = C_2H_3(+ M)$	$k_\infty\ 1.57 \times 10^{13}$	0	2719	(Marinov et al., 1995)
		$k_0\ 1.59 \times 10^{39}$	-7.27	6577	
		$F_{cent} = \exp(-T/2500\ K)$			
84	$C_2H_3 + H = C_2H_2 + H_2$	3.00×10^{13}	0	0	(Heinemann et al., 1986)
85	$C_2H_3 + O = CH_2CO + H$	9.60×10^{13}	0	0	(Tsang and Hampson, 1986)
86	$C_2H_3 + OH = C_2H_2 + H_2O$	3.00×10^{13}	0	0	(Tsang and Hampson, 1986)
87	$C_2H_3 + OH = CH_3HCO$	3.00×10^{13}	0	0	(Tsang and Hampson, 1986)
88	$C_2H_3 + O_2 = CH_2O + HCO$	4.48×10^{26}	-4.55	5480	(Westmoreland, 1992)
89	$C_2H_3 + O_2 = 2HCO + H$	3.27×10^{23}	-3.94	5010	(Westmoreland, 1992)
90	$C_2H_3 + HO_2 = CH_2CO + OH + H$	3.00×10^{13}	0	0	(Tsang and Hampson, 1986)
91	$C_2H_3 + CH_3 = C_2H_2 + CH_4$	3.90×10^{11}	0	0	(Tsang and Hampson, 1986)
92	$C_2H_3 + C_2H_3 = C_2H_4 + C_2H_2$	9.60×10^{11}	0	0	(Tsang and Hampson, 1986)
93	$C_2H_4(+M) = C_2H_2 + H_2(+M)$	$k_\infty\ 7.94 \times 10^{12}$	0.44	88760	(Tsang and Hampson, 1986)
		$k_0\ 6.10 \times 10^{06}$	2.88	67200	
94	$C_2H_3 + H(+ M) = C_2H_4(+ M)$	$k_\infty\ 6.08 \times 10^{12}$	0.27	280	(Bowman et al., 1996)
		$k_0\ 1.40 \times 10^{30}$	-3.86	3320	
		$F_{cent} = (1 - 0.782)\exp(- T/208\ K) + 0.782\exp(- T/2663\ K) + \exp(- 6095\ K/T)$			
95	$C_2H_4 + H = C_2H_3 + H_2$	1.32×10^{06}	2.53	12240	(Tsang and Hampson, 1986)
96	$C_2H_4 + O = CH_3 + HCO$	1.32×10^{08}	1.55	427	(Tsang and Hampson, 1986)
97	$C_2H_4 + OH = C_2H_3 + H_2O$	2.02×10^{13}	0	5955	(Tully, 1988)
98	$C_2H_4 + O_2 = C_2H_3 + HO_2$	4.22×10^{13}	0	57600	(Tsang and Hampson, 1986)
99	$C_2H_4 + CH_3 = C_2H_3 + CH_4$	6.62×10^{00}	3.70	9500	(Tsang and Hampson, 1986)

C_2H_5/C_2H_6

	Reaction	A	n	E	Reference
100	$C_2H_5(+ M) = C_2H_4 + H(+ M)$	$k_\infty\ 4.90 \times 10^{09}$	1.19	37200	(Tsang and Hampson, 1986)
		$k_0\ 5.10 \times 10^{04}$	-13.96	60100	

TABLE II (Continued)

	Reaction	A (cm-mol-s)	n	E_a (cal/mol)	Reference
101	$C_2H_5 + O = CH_3HCO + H$	9.60×10^{13}	0	0	(Tsang and Hampson, 1986)
102	$C_2H_5 + OH = C_2H_4 + H_2O$	2.40×10^{13}	0	0	(Tsang and Hampson, 1986)
103	$C_2H_5 + OH = CH_3 + H + CH_2O$	2.40×10^{13}	0	0	(Tsang and Hampson, 1986)
104	$C_2H_5 + O_2 = C_2H_4 + HO_2$	8.43×10^{11}	0	3874	(Tsang and Hampson, 1986)
105	$C_2H_5 + HO_2 \rightarrow CH_3 + CH_2O + OH$	2.40×10^{13}	0	0	(Tsang and Hampson, 1986)
106	$C_2H_5 + HO_2 = C_2H_4 + H_2O_2$	3.00×10^{11}	0	0	(Tsang and Hampson, 1986)
107	$C_2H_5 + C_2H_5 = C_2H_4 + C_2H_6$	1.40×10^{12}	0	0	(Tsang and Hampson, 1986)
108	$C_2H_6 = C_2H_5 + H$	2.08×10^{38}	-7.08	106500	(Dagaut et al., 1991)
109	$C_2H_6 + H = C_2H_5 + H_2$	5.42×10^{02}	3.50	5166	(Clark and Dove, 1973)
110	$C_2H_6 + O = C_2H_5 + OH$	1.20×10^{12}	0.60	7311	(Tsang and Hampson, 1986)
111	$C_2H_6 + OH = C_2H_5 + H_2O$	5.13×10^{06}	2.06	854	(Tully et al., 1986)
112	$C_2H_6 + O_2 = C_2H_5 + HO_2$	4.00×10^{13}	0	50900	(Walker, 1975)
113	$C_2H_6 + HO_2 = C_2H_5 + H_2O_2$	2.94×10^{11}	0	14940	(Walker, 1977)
114	$C_2H_6 + CH_3 = C_2H_5 + CH_4$	5.48×10^{-01}	4.00	8284	(Clark and Dove, 1973)
115	$C_2H_6 + C_2H_3 = C_2H_5 + C_2H_4$	6.00×10^{02}	3.30	10500	(Tsang and Hampson, 1986)
116	$C_2H_6 + C_3H_5 = C_2H_5 + C_3H_6$	2.35×10^{02}	3.30	19830	(Tsang and Hampson, 1986)
	CH₃CO/CH₂CO/CH₃HCO				
117	$CH_2CO + M = CH_2 + CO + M$	3.60×10^{15}	0	59270	(Warnatz, 1984b)
118	$CH_2CO + H = CH_3 + CO$	7.00×10^{12}	0	3000	(Warnatz, 1984b)
119	$CH_2CO + O = HCO + HCO$	2.00×10^{13}	0	2294	(Warnatz, 1984b)
120	$CH_2CO + OH = CH_2O + HCO$	1.00×10^{13}	0	0	(Tsang and Hampson, 1986)
121	$CH_3CO(+M) = CH_3 + CO(+M)$	$k_\infty\ 1.20 \times 10^{22}$ $k_0\ 8.73 \times 10^{42}$	-3.04 -8.62	18800 22400	(Tsang and Hampson, 1986)
122	$CH_3CO + H = CH_3 + HCO$	9.60×10^{13}	0	0	(Tsang and Hampson, 1986)
123	$CH_3CO + O = CH_3 + CO_2$	9.60×10^{12}	0	0	(Tsang and Hampson, 1986)

No.	Reaction	A	n	E	Reference
124	$CH_3CO + OH = CH_2CO + H_2O$	1.20×10^{13}	0	0	(Tsang and Hampson, 1986)
125	$CH_3CO + OH \rightarrow CH_3 + CO + OH$	3.00×10^{13}	0	0	(Tsang and Hampson, 1986)
126	$CH_3CO + HO_2 \rightarrow CH_3 + CO_2 + OH$	3.00×10^{13}	0	0	(Tsang and Hampson, 1986)
127	$CH_3HCO = CH_3 + HCO$	7.08×10^{15}	0	81760	(Colket et al., 1975)
128	$CH_3HCO + H = CH_3CO + H_2$	4.00×10^{13}	0	4207	(Warnatz, 1981)
129	$CH_3HCO + O = CH_3CO + OH$	5.00×10^{12}	0	1793	(Warnatz, 1981)
130	$CH_3HCO + OH = CH_3CO + H_2O$	1.00×10^{13}	0	0	(Kaiser et al., 1986)
131	$CH_3HCO + O_2 = CH_3CO + HO_2$	2.00×10^{13}	0.50	42200	(Colket et al., 1977)
132	$CH_3HCO + HO_2 = CH_3CO + H_2O_2$	1.70×10^{12}	0	10700	(Warnatz, 1981)
133	$CH_3HCO + CH_3 = CH_3CO + CH_4$	1.74×10^{12}	0	8440	(Lin and Laidler, 1968)

C_3H_3/C_3H_4

No.	Reaction	A	n	E	Reference
134	$C_3H_3 + O = CH_2O + C_2H$	2.00×10^{13}	0	0	(Miller and Bowman, 1989)
135	$C_3H_3 + O_2 = CH_2CO + HCO$	3.01×10^{10}	0	2870	(Slagle and Gutman, 1986)
136	$C_3H_3 + CH_3 = C_2H_5 + C_2H$	1.00×10^{13}	0	37500	(Wu and Kern, 1987)
137	$C_3H_3 + CH_3 \rightarrow C_4H_6$	5.00×10^{12}	0	0	(Wu and Kern, 1987)
138	$2C_3H_3 = C_6H_6$	3.00×10^{11}	0	0	(Wu and Kern, 1987)
139	$2C_3H_3 = 3C_2H_2$	5.00×10^{11}	0	0	(Wu and Kern, 1987)
140	$C_3H_4 + M = C_3H_3 + H + M$	1.00×10^{17}	0	70000	(Wu and Kern, 1987)
141	$C_3H_4 + H = C_3H_3 + H_2$	1.00×10^{12}	0	1500	(Wu and Kern, 1987)
142	$C_3H_4 + O = CH_2O + C_2H_2$	3.00×10^{-03}	4.61	-4243	(Dagaut et al., 1990)
143	$C_3H_4 + O = CO + C_2H_4$	9.00×10^{-03}	4.61	-4243	(Dagaut et al., 1990)
144	$C_3H_4 + OH = C_3H_3 + H_2O$	1.45×10^{13}	0	4170	(Liu et al., 1988)
145	$C_3H_4 + OH = CH_2CO + CH_3$	3.12×10^{12}	0	-397	(Dagaut et al., 1990)
146	$C_3H_4 + O_2 = C_3H_3 + HO_2$	4.00×10^{13}	0	61500	(Dagaut et al., 1990)
147	$C_3H_4 + HO_2 \rightarrow CH_2CO + CH_2 + OH$	4.00×10^{12}	0	19000	(Dagaut et al., 1990)
148	$C_3H_4 + CH_3 = C_3H_3 + CH_4$	2.00×10^{12}	0	7700	(Wu and Kern, 1987)
149	$C_3H_4 + C_3H_3 = C_6H_6 + H$	2.20×10^{11}	0	2000	(Wu and Kern, 1987)

C_2H_5HCO

No.	Reaction	A	n	E	Reference
150	$C_2H_5HCO + H \rightarrow C_2H_5 + CO + H_2$	4.00×10^{09}	1.16	2400	g
151	$C_2H_5HCO + O \rightarrow C_2H_5 + CO + OH$	6.00×10^{12}	0	1900	g
152	$C_2H_5HCO + OH \rightarrow C_2H_5 + CO + H_2O$	8.00×10^{12}	0	0	g

TABLE II (Continued)

	Reaction	A (cm-mol-s)	n	E_a (cal/mol)	Reference
C₃H₅/C₃H₆					
153	$C_3H_5 = C_3H_4 + H$	1.50×10^{11}	0.84	59810	(Tsang and Walker, 1992)
154	$C_3H_5 + H = C_3H_4 + H_2$	1.80×10^{13}	0	0	(Tsang, 1991)
155	$C_3H_5 + O = C_2H_3HCO + H$	6.02×10^{13}	0	0	(Tsang, 1991)
156	$C_3H_5 + OH = C_3H_4 + H_2O$	6.02×10^{12}	0	0	(Tsang, 1991)
157	$C_3H_5 + O_2 = C_3H_4 + HO_2$	1.33×10^{07}	0	0	(Slagle et al., 1986) h
158	$C_3H_5 + HO_2 \rightarrow C_3H_3 + CH_2O + OH$	6.72×10^{11}	0	0	
159	$C_3H_5 + HCO = C_3H_6 + CO$	6.00×10^{13}	0	0	(Tsang, 1991)
160	$C_3H_5 + CH_3 = C_3H_4 + CH_4$	3.00×10^{12}	−0.32	−262	(Tsang, 1991)
161	$C_3H_5 + C_2H_3 = C_3H_6 + C_2H_2$	4.80×10^{12}	0	0	(Tsang, 1991)
162	$C_3H_5 + C_2H_5 = C_3H_4 + C_2H_4$	2.40×10^{12}	0	0	(Tsang, 1991)
163	$C_3H_5 + C_2H_5 = C_3H_6 + C_2H_4$	2.60×10^{12}	0	−131	(Tsang, 1991)
164	$C_3H_5 + C_2H_5 = C_3H_4 + C_2H_6$	9.60×10^{11}	0	−131	(Tsang, 1991)
165	$2C_3H_5 = C_3H_4 + C_3H_6$	8.43×10^{10}	0	−263	(Tsang, 1991)
166	$2C_3H_5 = 1,5\text{-}C_6H_{10}$	1.02×10^{13}	0	−263	(Dagaut et al., 1990)
167	$C_3H_6 = C_2H_3 + CH_3$	1.10×10^{21}	−1.20	97710	(Tsang, 1991)
168	$C_3H_6 = C_3H_5 + H$	2.50×10^{15}	0	87580	(Tsang, 1991)
169	$C_3H_6 + H = C_3H_5 + H_2$	1.73×10^{05}	2.50	2490	(Tsang, 1991)
170	$C_3H_6 + H = C_2H_4 + CH_3$	1.33×10^{13}	0	3261	(Tsang, 1991)
171	$C_3H_6 + O \rightarrow CH_2CO + CH_3 + H$	7.70×10^{07}	1.66	634	(Tsang, 1991)
172	$C_3H_6 + O = C_2H_5 + HCO$	3.43×10^{07}	1.66	−193	(Tsang, 1991)
173	$C_3H_6 + O = C_3H_5 + OH$	1.75×10^{11}	0.70	5883	(Tsang, 1991)
174	$C_3H_6 + OH = C_3H_5 + H_2O$	3.12×10^{06}	2.00	−298	(Tsang, 1991)
175	$C_3H_6 + O_2 = C_3H_5 + HO_2$	6.02×10^{13}	0	47600	(Tsang, 1991)
176	$C_3H_6 + HO_2 = C_3H_5 + H_2O_2$	9.64×10^{03}	2.60	13900	(Tsang, 1991)
177	$C_3H_6 + CH_3 = C_3H_5 + CH_4$	2.22×10^{00}	3.50	5675	(Tsang, 1991)
178	$C_3H_6 + C_2H_3 = C_3H_5 + C_2H_4$	2.22×10^{00}	3.50	4679	(Tsang, 1991)

C_4H_6

No.	Reaction	A	n	E	Reference
179	$C_4H_6 \rightarrow C_3H_3 + C_2H_3 + H$	1.58×10^{16}	0	110000	(Dean, 1985)
180	$C_4H_6 = C_2H_3 + C_2H_3$	1.80×10^{13}	0	85000	(Rao et al., 1988)
181	$C_4H_6 + H = C_2H_5 + C_2H_4$	5.00×10^{11}	0	0	(Kiefer et al., 1985)
182	$C_4H_6 + H \rightarrow H_2 + C_2H_2 + C_2H_5$	6.30×10^{10}	0.70	6000	(Weissman and Benson, 1988)
183	$C_4H_6 + OH \rightarrow HCO + H + C_3H_5$	5.00×10^{12}	0	0	g
184	$C_4H_6 + OH \rightarrow C_2H_3HCO + CH_3$	5.00×10^{12}	0	0	g
185	$C_4H_6 + CH_3 \rightarrow CH_4 + C_3H_2 + C_2H_3$	7.00×10^{13}	0	18500	(Kern et al., 1988)

$1\text{-}C_4H_8$

No.	Reaction	A	n	E	Reference
186	$1\text{-}C_4H_8 = C_3H_5 + CH_3$	1.00×10^{16}	0	73000	(Dean, 1985)
187	$1\text{-}C_4H_8 + H = C_2H_4 + C_2H_5$	7.23×10^{12}	0	1302	(Tsang, 1991)ʲ
188	$1\text{-}C_4H_8 + H = C_3H_6 + CH_3$	7.23×10^{12}	0	1302	(Tsang, 1991)ʲ
189	$1\text{-}C_4H_8 + H \rightarrow H_2 + C_4H_6 + H$	1.15×10^{05}	2.50	2490	j
190	$1\text{-}C_4H_8 + H \rightarrow H_2 + C_2H_5 + C_2H_4$	6.60×10^{05}	2.54	6760	j
191	$1\text{-}C_4H_8 + O \rightarrow OH + C_4H_6 + H$	1.16×10^{11}	0.70	5880	j
192	$1\text{-}C_4H_8 + O \rightarrow OH + C_2H_3 + C_2H_4$	9.60×10^{04}	2.68	3720	j
193	$1\text{-}C_4H_8 + OH \rightarrow H_2O + C_4H_6 + H$	2.08×10^{06}	2.00	-298	j
194	$1\text{-}C_4H_8 + OH \rightarrow H_2O + C_2H_5 + C_2H_4$	1.58×10^{07}	1.80	930	j
195	$1\text{-}C_4H_8 + CH_3 \rightarrow CH_4 + C_4H_6 + H$	1.48×10^{00}	3.50	5670	j

$1\text{-}C_5H_{10}$

No.	Reaction	A	n	E	Reference
196	$1\text{-}C_5H_{10} = C_3H_5 + C_2H_5$	1.00×10^{16}	0	71340	(Tsang, 1978b)
197	$1\text{-}C_5H_{10} = C_3H_6 + C_2H_4$	3.16×10^{12}	0	57040	(Tsang, 1978b)
198	$1\text{-}C_5H_{10} + H = 2C_2H_4 + CH_3$	7.23×10^{12}	0	1302	(Tsang, 1991)ʲ
199	$1\text{-}C_5H_{10} + H = C_3H_6 + C_2H_5$	7.23×10^{12}	0	1302	(Tsang, 1991)ʲ
200	$1\text{-}C_5H_{10} + H \rightarrow H_2 + C_4H_6 + CH_3$	1.15×10^{05}	2.50	2490	j
201	$1\text{-}C_5H_{10} + H \rightarrow H_2 + C_3H_5 + C_2H_5$	6.60×10^{05}	2.54	6760	j
202	$1\text{-}C_5H_{10} + H \rightarrow H_2 + C_3H_6 + C_2H_3$	1.30×10^{06}	2.40	4470	j
203	$1\text{-}C_5H_{10} + O \rightarrow OH + C_4H_6 + CH_3$	1.16×10^{11}	0.70	5880	j
204	$1\text{-}C_5H_{10} + O \rightarrow OH + C_3H_5 + C_2H_5$	9.60×10^{04}	2.68	3720	j
205	$1\text{-}C_5H_{10} + O \rightarrow OH + C_3H_6 + C_2H_3$	4.76×10^{04}	2.71	2110	j
206	$1\text{-}C_5H_{10} + OH \rightarrow H_2O + C_4H_6 + CH_3$	2.08×10^{06}	2.00	-298	j

T. J. HELD *et al.*

TABLE II (Continued)

	Reaction	A (cm-mol-s)	n	E_a (cal/mol)	Reference
207	$1\text{-}C_5H_{10}+OH\rightarrow H_2O+C_2H_4+C_3H_5$	1.58×10^{07}	1.80	930	j
208	$1\text{-}C_5H_{10}+OH\rightarrow H_2O+C_3H_6+C_2H_5$	7.08×10^{06}	1.90	160	j
209	$1\text{-}C_5H_{10}+CH_3\rightarrow CH_4+C_4H_6+CH_3$	1.48×10^{00}	3.50	5670	j
$1\text{-}C_6H_{12}$					
210	$1\text{-}C_6H_{12}=2C_3H_6$	3.98×10^{12}	0	57430	(Tsang, 1978a)
211	$1\text{-}C_6H_{12}\rightarrow C_3H_5+C_2H_4+CH_3$	7.94×10^{15}	0	70740	(Tsang, 1978a)
212	$1\text{-}C_6H_{12}+H\rightarrow C_3H_6+C_2H_4+CH_3$	7.23×10^{12}	0	1302	(Tsang, 1991a)
213	$1\text{-}C_6H_{12}+H\rightarrow 2C_2H_4+C_2H_5$	7.23×10^{12}	0	1302	(Tsang, 1991a)
214	$1\text{-}C_6H_{12}+H\rightarrow H_2+C_4H_6+C_2H_5$	1.15×10^{05}	2.50	2490	j
215	$1\text{-}C_6H_{12}+H\rightarrow H_2+2C_2H_4+C_2H_3$	6.60×10^{05}	2.54	6760	j
216	$1\text{-}C_6H_{12}+H\rightarrow H_2+C_3H_6+C_3H_5$	1.30×10^{06}	2.40	4470	j
217	$1\text{-}C_6H_{12}+H\rightarrow H_2+C_2H_3+1\text{-}C_4H_8$	1.30×10^{06}	2.40	4470	j
218	$1\text{-}C_6H_{12}+O\rightarrow OH+C_4H_6+C_3H_5$	1.16×10^{11}	0.70	5880	j
219	$1\text{-}C_6H_{12}+O\rightarrow OH+2C_2H_4+C_2H_3$	9.60×10^{04}	2.68	3720	j
220	$1\text{-}C_6H_{12}+O\rightarrow OH+C_3H_6+C_3H_5$	4.76×10^{04}	2.71	2110	j
221	$1\text{-}C_6H_{12}+O\rightarrow OH+C_2H_3+1\text{-}C_4H_8$	4.76×10^{04}	2.71	2110	j
222	$1\text{-}C_6H_{12}+OH\rightarrow H_2O+C_4H_6+C_2H_5$	2.08×10^{06}	2.00	-298	j
223	$1\text{-}C_6H_{12}+OH\rightarrow H_2O+2C_2H_4+C_2H_3$	1.58×10^{07}	1.80	930	j
224	$1\text{-}C_6H_{12}+OH\rightarrow H_2O+C_3H_6+C_3H_5$	7.08×10^{06}	1.90	160	j
225	$1\text{-}C_6H_{12}+OH\rightarrow H_2O+C_2H_3+1\text{-}C_4H_8$	7.08×10^{06}	1.90	160	j
226	$1\text{-}C_6H_{12}+CH_3\rightarrow CH_4+C_4H_6+C_2H_5$	1.48×10^{00}	3.50	5670	j
$n\text{-}C_7H_{16}$ decomposition					
227	$C_7H_{16}\rightarrow H+3C_2H_4+CH_3$	1.80×10^{16}	0	100600	(Dean, 1985)
228	$C_7H_{16}\rightarrow H+C_3H_6+C_2H_4+C_2H_5$	1.20×10^{16}	0	98090	(Dean, 1985)
229	$C_7H_{16}\rightarrow H+1\text{-}C_4H_8+C_2H_4+CH_3$	1.20×10^{16}	0	98090	(Dean, 1985)
230	$C_7H_{16}\rightarrow H+1\text{-}C_5H_{10}+C_2H_5$	6.00×10^{15} $+4.00\times10^{17}$	0 0	98090 87300	(Dean, 1985) (Dean, 1985)
231	$C_7H_{16}\rightarrow H+CH_3+2C_2H_4+C_2H_5$	4.00×10^{17} $+2.00\times10^{17}$	0 0	85400 84900	

$nC_7H_{16} \rightarrow 1\text{-}C_7H_{15} \rightarrow$ products

No.	Reaction	A	n	E_a	Reference
232	$C_7H_{16} + H \rightarrow H_2 + 3C_2H_4 + CH_3$	1.32×10^{06}	2.54	6760	j
233	$C_7H_{16} + O \rightarrow OH + 3C_2H_4 + CH_3$	2.88×10^{06}	2.40	5505	(Cohen and Westberg, 1986)
234	$C_7H_{16} + OH \rightarrow H_2O + 3C_2H_4 + CH_3$	1.74×10^{07}	1.80	974	(Cohen, 1991)
235	$C_7H_{16} + O_2 \rightarrow HO_2 + 3C_2H_4 + CH_3$	3.98×10^{13}	0	50900	j
236	$C_7H_{16} + HO_2 \rightarrow H_2O_2 + 3C_2H_4 + CH_3$	4.76×10^{04}	2.55	16500	j
237	$C_7H_{16} + CH_3 \rightarrow CH_4 + 3C_2H_4 + CH_3$	9.06×10^{-01}	3.46	5480	j
238	$C_7H_{16} + C_2H_5 \rightarrow C_3H_6 + 3C_2H_4 + CH_3$	2.35×10^{02}	3.30	19800	j

$nC_7H_{16} \rightarrow 2\text{-}C_7H_{15} \rightarrow$ products

No.	Reaction	A	n	E_a	Reference
239	$C_7H_{16} + H \rightarrow H_2 + C_3H_6 + C_2H_4 + C_2H_5$	2.60×10^{06}	2.40	4470	j
240	$C_7H_{16} + O \rightarrow OH + C_3H_6 + C_2H_4 + C_2H_5$	2.76×10^{05}	2.60	1910	(Cohen and Westberg, 1986)
241	$C_7H_{16} + OH \rightarrow H_2O + C_3H_6 + C_2H_4 + C_2H_5$	3.80×10^{06}	2.00	−596	(Cohen, 1991)
242	$C_7H_{16} + O_2 \rightarrow HO_2 + C_3H_6 + C_2H_4 + C_2H_5$	7.92×10^{13}	0	47590	j
243	$C_7H_{16} + HO_2 \rightarrow H_2O_2 + C_3H_6 + C_2H_4 + C_2H_5$	1.93×10^{04}	2.60	13900	j
244	$C_7H_{16} + CH_3 \rightarrow CH_4 + C_3H_6 + C_2H_4 + C_2H_5$	4.27×10^{11}	0	10500	j
245	$C_7H_{16} + C_2H_5 \rightarrow 2C_3H_6 + C_2H_4 + C_2H_5$	1.57×10^{02}	3.30	18200	(Tsang, 1991)[m]

$nC_7H_{16} \rightarrow 3\text{-}C_7H_{15} \rightarrow$ products[n]

No.	Reaction	A	n	E_a	Reference
246	$C_7H_{16} + H \rightarrow H_2 + 1\text{-}C_4H_8 + C_2H_4 + CH_3$	2.08×10^{06}	2.40	4470	j
247	$C_7H_{16} + H \rightarrow H_2 + 1\text{-}C_6H_{12} + CH_3$	5.20×10^{05}	2.40	4470	j
248	$C_7H_{16} + O \rightarrow OH + 1\text{-}C_4H_8 + C_2H_4 + CH_3$	2.21×10^{05}	2.60	1910	(Cohen and Westberg, 1986)[j]
249	$C_7H_{16} + O \rightarrow OH + 1\text{-}C_6H_{12} + CH_3$	5.50×10^{04}	2.60	1910	(Cohen and Westberg, 1986)[j]
250	$C_7H_{16} + OH \rightarrow H_2O + 1\text{-}C_4H_8 + C_2H_4 + CH_3$	3.50×10^{06}	2.00	−1312	(Cohen, 1991)
251	$C_7H_{16} + OH \rightarrow H_2O + 1\text{-}C_6H_{12} + CH_3$	8.74×10^{05}	2.00	−1312	(Cohen, 1991)
252	$C_7H_{16} + O_2 \rightarrow HO_2 + 1\text{-}C_4H_8 + C_2H_4 + CH_3$	6.34×10^{13}	0	47600	j
253	$C_7H_{16} + O_2 \rightarrow HO_2 + 1\text{-}C_6H_{12} + CH_3$	1.58×10^{13}	0	47600	j
254	$C_7H_{16} + HO_2 \rightarrow H_2O_2 + 1\text{-}C_4H_8 + C_2H_4 + CH_3$	1.54×10^{04}	2.60	13900	j
255	$C_7H_{16} + HO_2 \rightarrow H_2O_2 + 1\text{-}C_6H_{12} + CH_3$	3.86×10^{03}	2.60	13900	j

TABLE II (Continued)

Reaction	A (cm-mol-s)	n	E_a (cal/mol)	Reference
256	$C_7H_{16} + CH_3 \rightarrow CH_4 + 1-C_4H_8 + C_2H_4 + CH_3$	2.41×10^{03}	3.46	5480	j
257	$C_7H_{16} + CH_3 \rightarrow CH_4 + 1-C_6H_{12} + CH_3$	6.02×10^{-01}	3.46	5480	j
258	$C_7H_{16} + C_2H_5 \rightarrow C_3H_6 + 1-C_4H_8 + C_2H_4 + CH_3$	1.25×10^{02}	3.30	18200	j
259	$C_7H_{16} + C_3H_5 \rightarrow C_3H_6 + 1-C_6H_{12} + CH_3$	3.13×10^{01}	3.30	18200	j

$nC_7H_{16} \rightarrow 4\text{-}C_3H_{15} \rightarrow$ products

Reaction	A (cm-mol-s)	n	E_a (cal/mol)	Reference
260	$C_7H_{16} + H \rightarrow H_2 + 1-C_5H_{10} + C_2H_5$	1.30×10^{06}	2.40	4470	j
261	$C_7H_{16} + O \rightarrow OH + 1-C_5H_{10} + C_2H_5$	1.38×10^{05}	2.60	1910	(Cohen and Westberg, 1986)[a]
262	$C_7H_{16} + OH \rightarrow H_2O + 1-C_5H_{10} + C_2H_5$	4.37×10^{06}	2.00	-1312	(Cohen, 1991)
263	$C_7H_{16} + O_2 \rightarrow HO_2 + 1-C_5H_{10} + C_2H_5$	3.96×10^{13}	0	47600	j
264	$C_7H_{16} + HO_2 \rightarrow H_2O_2 + 1-C_5H_{10} + C_2H_5$	9.64×10^{03}	2.60	13900	j
265	$C_7H_{16} + CH_3 \rightarrow CH_4 + 1-C_5H_{10} + C_2H_5$	1.51×10^{00}	3.46	5480	j
266	$C_7H_{16} + C_3H_5 \rightarrow C_3H_6 + 1-C_5H_{10} + C_2H_5$	7.83×10^{01}	3.30	18160	j

Notes for Table II

[a] Reversible reactions designated by " $=$ ", non-reversible by " $\rightarrow$ "

[b] Enhanced third body efficiencies (relative to N_2): $\eta_{H_2} = 2.5, \eta_{H_2O} = 12, \eta_{CO} = 1.9, \eta_{CO_2} = 3.8, \eta_{Ar} = 0$. Unless otherwise specified, all species are assumed to have a third body efficiency of 1.0

[c] Enhanced third body efficiencies (relative to N_2): $\eta_{H_2} = 2.5, \eta_{H_2O} = 12, \eta_{CO} = 1.9, \eta_{CO_2} = 3.8, \eta_{Ar} = 0.75$

[d] Enhanced third body efficiencies (relative to N_2): $\eta_{H_2} = 2.5, \eta_{H_2O} = 6.3, \eta_{CO} = 1.9, \eta_{CO_2} = 3.8, \eta_{Ar} = 0.38$

[e] Pressure dependent reaction — k_0 and k_∞ refer to low and high pressure limits, respectively. Reactions with specified F_{cent} parameters use the Troe form, all others use the Lindemann expression

[f] Enhanced third body efficiencies (relative to N_2): $\eta_{H_2} = 2.5, \eta_{H_2O} = 12, \eta_{CO} = 1.9, \eta_{CO_2} = 3.8, \eta_{Ar} = 0.87$

[g] Estimated

[h] Present work

[i] value for C_3H_6

[j] rate constants were assigned by comparison to prototypical hydrocarbon species, accounting for number of available sites, and type of C-H bond involved (primary, secondary and allylic). See Table 3 for the rate constants per available H-atom

[k] literature value $\times 2$ to improve agreement with pyrolysis data

[l] literature rate $\times 0.4$ to account for number of possible sites

[m] value for secondary C_3H_8 abstraction

[n] 80% of 3-C_7H_{15} decomposition assigned to 1-C_4H_8 + 1-C_3H_7, remainder to 1-C_6H_{12} + CH_3

[o] literature rate $\times 0.2$ to account for number of possible sites

TABLE III Abstraction reaction rate constants

Prototype reaction	A (per site) (cm-mol-s)	n	E_a (cal/mol)	Reference
Primary C-H sites				
$C_3H_8 + H = H_2 + n\text{-}C_3H_7$	2.20×10^{05}	2.54	6760	(Tsang, 1988)
$C_3H_8 + O = OH + n\text{-}C_3H_7$	3.20×10^{04}	2.68	3720	(Tsang, 1988)
$C_3H_8 + OH = H_2O + n\text{-}C_3H_7$	5.27×10^{06}	1.80	930	(Tsang, 1988)
$C_3H_8 + O_2 = HO_2 + n\text{-}C_3H_7$	6.62×10^{12}	0	50900	(Tsang, 1988)
$C_3H_8 + HO_2 = H_2O_2 + n\text{-}C_3H_7$	7.93×10^{03}	2.55	16500	(Tsang, 1988)
$C_3H_8 + CH_3 = CH_4 + n\text{-}C_3H_7$	1.00×10^{02}	3.65	7150	(Tsang, 1988)
$C_3H_8 + C_3H_5 = C_3H_6 + n\text{-}C_3H_7$	3.91×10^{01}	3.30	19800	(Tsang, 1988)
Secondary C-H sites				
$C_3H_8 + H = H_2 + i\text{-}C_3H_7$	6.50×10^{05}	2.40	4470	(Tsang, 1988)
$C_3H_8 + O = OH + i\text{-}C_3H_7$	2.38×10^{04}	2.71	2110	(Tsang, 1988)
$C_3H_8 + OH = H_2O + i\text{-}C_3H_7$	3.54×10^{06}	1.90	160	(Tsang, 1988)
$C_3H_8 + O_2 = HO_2 + i\text{-}C_3H_7$	1.98×10^{13}	0	47600	(Tsang, 1988)
$C_3H_8 + HO_2 = H_2O_2 + i\text{-}C_3H_7$	4.82×10^{03}	2.60	13900	(Tsang, 1988)
$C_3H_8 + CH_3 = CH_4 + i\text{-}C_3H_7$	7.53×10^{-01}	3.46	5480	(Tsang, 1988)
$C_3H_8 + C_3H_5 = C_3H_6 + i\text{-}C_3H_7$	3.91×10^{01}	3.30	18200	(Tsang, 1988)
Allylic C-H sites				
$C_3H_6 + H = H_2 + C_3H_5$	5.76×10^{04}	2.50	2490	(Tsang, 1991)
$C_3H_6 + O = OH + C_3H_5$	5.82×10^{10}	0.70	5880	(Tsang, 1991)
$C_3H_6 + OH = H_2O + C_3H_5$	1.04×10^{06}	2.00	-298	(Tsang, 1991)
$C_3H_6 + O_2 = HO_2 + C_3H_5$	2.00×10^{13}	0	4760	(Tsang, 1991)
$C_3H_6 + HO_2 = H_2O_2 + C_3H_5$	3.21×10^{03}	2.60	13900	(Tsang, 1991)
$C_3H_6 + CH_3 = CH_4 + C_3H_5$	7.39×10^{-01}	3.50	5670	(Tsang, 1991)

products listed in the bottom row of Table I. Because no other reaction channels are considered for the alkyl radicals, those species could be eliminated from the mechanism by writing the abstraction/decomposition sequence as an overall reaction. In the following example, the sequence:

$$C_7H_{16} + OH \rightarrow 2\text{-}C_7H_{15} + H_2O$$

$$2\text{-}C_7H_{15} \rightarrow C_3H_6 + 1\text{-}C_4H_9$$

$$1\text{-}C_4H_9 \rightarrow C_2H_4 + C_2H_5$$

is written:

$$C_7H_{16} + OH \rightarrow C_3H_6 + C_2H_4 + C_2H_5 + H_2O.$$
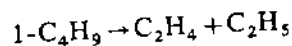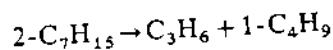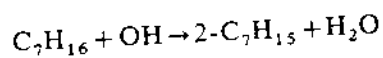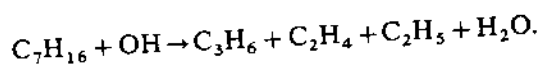
The large 1-olefins ($\geqslant C_4$) are treated in a simplified manner. Three types of reaction are considered—thermal decomposition, abstraction by an active

radical, and H-atom addition. Because of the resonant stability of the allyl radical (C_3H_5), the C-C bond one removed from the double bond, and C-H bonds at the carbon adjacent to the double bond, are relatively weak (e.g., $D(C-C) = 67$ kcal/mole for $1-C_4H_8 \rightarrow C_3H_5 + CH_3$, vs. 89 kcal/mole for $nC_4H_{10} \rightarrow nC_3H_7 + CH_3$). Thus, the primary thermal decomposition channel for 1-olefins yields allyl and an alkyl radical.

Abstraction reactions from the primary and secondary sites of the larger olefins (> C_3) are modeled in a similar manner as for *n*-heptane. The rate constants for abstraction from the allylic sites are estimated by analogy to allylic H-abstraction from the corresponding site of propene (Tsang, 1991) (Tab. III). Abstraction from the vinylic sites is assumed to be negligible. The subsequent alkyl and alkenyl radicals are also assumed to rapidly thermally decompose.

Addition of a hydrogen atom to either of the unsaturated carbon sites can be an important process in olefin pyrolysis and oxidation. The resulting excited alkyl radical is assumed to thermally decompose to β-scission products.

The submechanism for C_3H_6 and smaller species is a subset of a mechanism under development for comprehensive *n*-butane oxidation studies. The $C_1 - C_3$ submechanisms are compiled primarily from the reviews of Tsang *et al.* (1986; 1991). The $H_2/CO/O_2$ submechanism is from the work of Yetter and Dryer (1991) and Kim *et al.* (1994). The forward rate coefficients are listed in Table II. Reverse rate coefficients are calculated from the equilibrium constants, calculated from the thermodynamic properties listed in Table IV. The resulting set of differential equations was solved by the SENKIN (Lutz *et al.*, 1987), PSR (Glarborg *et al.*, 1986) and PREMIX (Kee *et al.*, 1985) codes of the Chemkin-II software package (Kee *et al.*, 1989). The final reaction mechanism consists of 266 reactions among 41 species.

FLOW REACTOR EXPERIMENTS

The experimental results presented in the following section were obtained using a variable-pressure flow reactor (Fig. 1). The experiment has been described in detail elsewhere (Held, 1993; Held and Dryer, 1994; Kim *et al.*, 1994); thus, only a summary is given here. An electrical resistance heater is used to preheat nitrogen carrier gas, which flows through a 10.16 cm diameter quartz tube. Oxygen is added to the flow upstream of the mixing zone, while pre-vaporized *n*-heptane (Aldrich, > 99%), diluted in approximately 6% of the total nitrogen flow, is added through the fuel injector at the mixing zone. The

TABLE IV   Thermodynamic data

Species	$\Delta H_{f,298}$	S_{298}	$c_{p,300}$	$c_{p,500}$	$c_{p,800}$	$c_{p,1000}$	$c_{p,1500}$	$c_{p,2000}$
H	52.07	27.38	4.97	4.97	4.97	4.97	4.97	4.97
O	59.53	38.45	5.23	5.08	5.02	5.00	4.98	4.98
OH	9.32	43.88	7.15	7.07	7.13	7.33	7.87	8.28
H_2	0.00	31.21	6.90	7.00	7.07	7.21	7.73	8.18
O_2	0.00	49.00	7.01	7.44	8.07	8.35	8.72	9.03
H_2O	−57.80	45.10	8.00	8.44	9.22	9.87	11.26	12.22
HO_2	3.00	54.43	8.36	9.48	10.75	11.37	12.34	12.90
H_2O_2	−32.53	55.65	10.41	12.34	14.29	15.21	16.85	17.88
CO	−26.42	47.21	6.95	7.14	7.61	7.95	8.41	8.67
CO_2	−94.05	51.08	8.91	10.65	12.32	12.99	13.93	14.44
CH	141.95	43.70	6.95	7.05	7.36	7.78	8.75	9.36
HCO	10.40	53.66	8.24	9.28	10.74	11.52	12.56	13.14
CH_2	92.45	46.70	8.24	8.88	9.93	10.56	11.73	12.53
CH_2O	−27.70	52.24	8.40	10.50	13.36	14.88	16.97	18.12
CH_3	34.82	46.37	9.23	10.83	12.87	14.12	16.27	17.55
CH_3O	3.90	54.60	9.08	12.43	16.63	18.60	21.51	23.26
CH_4	−17.90	44.46	8.43	11.14	15.00	17.25	20.63	22.58
HCCO	42.43	60.72	12.65	14.22	16.07	16.83	17.98	18.73
CH_2CO	−12.39	57.77	12.43	15.66	18.79	20.24	22.43	23.77
CH_3CO	−5.40	63.72	12.41	16.32	20.93	23.06	26.18	28.05
CH_3HCO	−39.49	63.02	13.24	18.30	24.16	26.87	30.86	33.25
C_2H	134.95	49.54	8.90	10.22	11.53	12.17	13.31	14.12
C_2H_2	54.17	48.00	10.62	13.08	15.27	16.30	18.27	19.51
C_2H_3	68.38	55.31	9.56	12.78	16.97	18.74	21.26	23.06
C_2H_4	12.53	52.36	10.23	14.94	20.04	22.50	26.21	28.32
C_2H_5	28.00	60.11	11.32	15.94	22.57	25.50	29.54	32.44
C_2H_6	−20.04	54.72	12.58	18.62	25.82	29.30	34.61	37.92
C_3H_3	76.46	59.88	14.00	18.32	22.35	24.22	27.25	28.98
C_2H_3HCO	−14.24	68.86	15.91	22.16	29.03	32.21	36.80	39.12
C_3H_4	45.21	54.88	14.12	19.78	25.43	27.99	31.93	34.15
C_3H_5	32.06	61.43	14.14	22.02	29.61	32.75	37.20	39.85
C_3H_6	4.89	61.49	15.46	22.72	30.77	34.51	40.12	43.53
C_4H_6	34.95	68.14	18.80	26.38	35.15	39.29	45.43	49.14
$1\text{-}C_4H_8$	−0.13	73.53	20.50	30.77	41.80	46.83	55.07	58.86
$1\text{-}C_5H_{10}$	−5.04	83.00	25.99	39.29	53.03	59.25	68.87	74.30
C_6H_6	19.81	64.34	19.91	33.24	45.85	51.03	58.29	62.93
$1,5\text{-}C_6H_{10}$	20.17	89.35	28.61	43.52	58.93	65.77	75.74	81.23
$1\text{-}C_6H_{12}$	−9.97	92.42	31.43	47.61	64.36	71.91	83.42	89.93
C_7H_{16}	−45.03	102.14	39.68	60.14	81.78	91.65	106.63	115.09
N_2	0.00	45.77	6.95	7.08	7.50	7.83	8.32	8.60
Ar	0.00	36.98	4.97	4.97	4.97	4.97	4.97	4.97

Units: $\Delta H_{f,298}$ (kcal/mol), S_{298} and c_p (cal/mol K)

n-heptane is pre-vaporized using a gas-assist atomization technique developed and described in Held (1993). The dilute reaction zone ($\approx 99\% N_2$) extends over approximately one meter in length, thus enabling temperature measurement and species sampling at varying distances from the point of injection. The
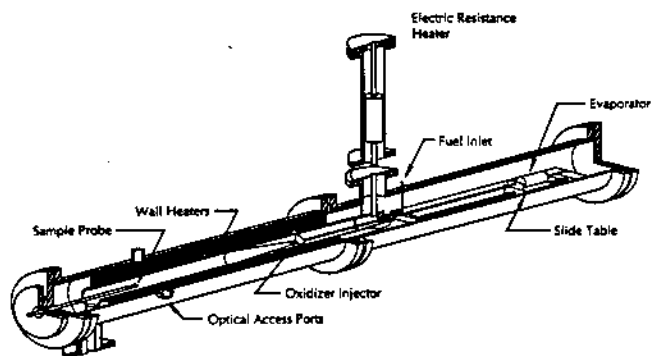
FIGURE 1 Cutaway view of variable pressure flow reactor.

time from injection is calculated at each location by integration of the centerline velocity profile and density:

$$\tau = \int_0^X \frac{dx}{U} = \int_0^X \frac{\rho(x) A_{\text{eff}}(x)}{\dot{m}} dx$$

where m is the measured mass flow rate, X is the distance from the point of fuel injection, $\rho(x)$ is the local density, and $A_{\text{eff}}(x)$ is the "effective cross-sectional area", defined as:

$$A_{\text{eff}}(x) \equiv \frac{U_{\text{plug}}}{U(x)} A(x)$$

where U_{plug} is the velocity calculated based on the plug flow assumption, $A(x)$ is the physical cross-sectional area of the reactor tupe, and $U(x)$ is the measured centerline velocity. The measured velocity is determined by pitot-static probe measurements in the reactor under cold-flow conditions, over the Reynolds number range nominally used in the experiments.

Flow rates are chosen such that thermal and species diffusion are negligible. Wall heaters surround the quartz tube to minimize the heat loss from the reacting mixture. The experiment may thus be approximately modeled as a zero-dimensional, isobaric and adiabatic system (Held, 1993). The initial conditions for these experiments are listed in Table V.

TABLE V   Initial conditions

Experiment	Pressure (atm)	Initial Temp. (K)	$X_{nC_7H_{16},i}$	$X_{O_2,i}$
Lean oxidation ($\phi = 0.79$)	3.0	940	0.00113	0.0158
Rich oxidation ($\phi = 2.27$)	3.0	1075	0.00163	0.0079
Pyrolysis	3.0	1085	0.00143	$< 10^{-5}$

The gas temperature is measured at the sampling location by a silica-coated Type-R thermocouple. A gas sample is continuously withdrawn from the reactor through a hot-water-cooled, stainless steel sampling probe. A small volume of the flowing sample gas is stored in two heated 16-position valves for subsequent analysis using a Hewlett Packard 5890 gas chromatograph with flame-ionization detection. Column switching (SGE MDS 2000) is used to separate C_1 through C_3 species on a PoraPlot-Q column, and C_4 and larger on a DB-5 column. In addition to the off-line gas chromatographic analysis, the continuous sample flow is analyzed by a number of on-line techniques. Oxygen is measured using an electrochemical analyzer (Infrared Industries, IR-2200), and carbon dioxide and carbon monoxide are measured by non-dispersive infrared analyzers (Horiba, PIR-2000). The carbon totals measured with the above instrumentation were constant to within ± 5% of the mean value.

FLOW REACTOR RESULTS

The measured species and temperature profiles for the oxidation and pyrolysis cases are shown as the symbols in Figures 2–4. In the oxidation cases, the pattern of fuel consumption, followed by small olefin formation, CO production and oxidation to CO_2 is consistent with the generalized hydrocarbon reaction mechanism that forms the basis for the present model development. No oxygenated species larger than formaldehyde could be detected. The pyrolysis experiment is remarkably similar to the rich oxidation case in both reaction rate (although the initial temperature is approximately 10 K higher in the pyrolysis case) and species distribution. These observations are consistent with high temperature oxidation characteristics–direct oxidation of the fuel or conjugate alkyl radicals is insignificant. This situation is in contrast to lower temperature studies in which large amounts of large oxygenated hydrocarbons
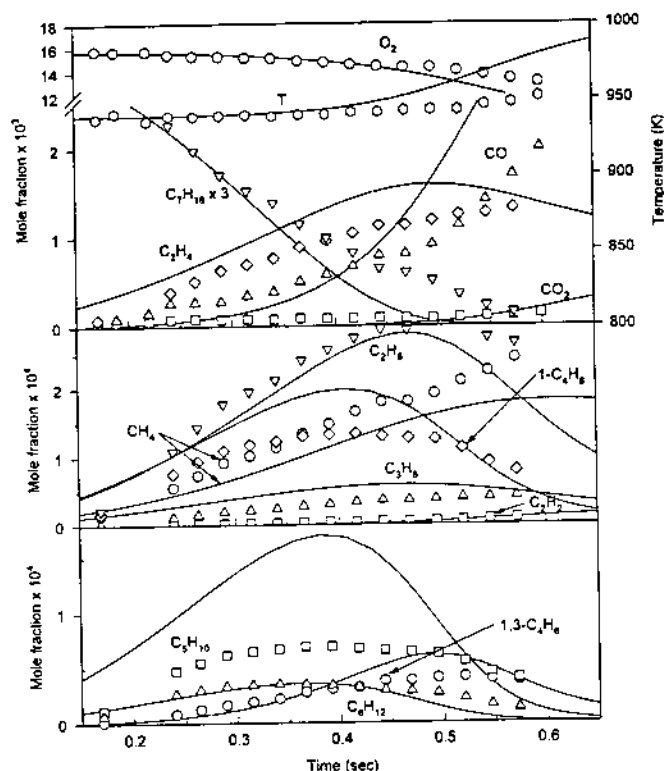
FIGURE 2   Measured (symbols) and calculated (lines) species and temperature profiles for lean n-heptane oxidation. Data have been shifted +0.15 sec to minimize RMS difference between calculated and measured nC_7H_{16} profiles.

are detected, and the overall reaction rate is significantly affected by the presence of molecular oxygen (Westbrook and Pitz, 1984; Dryer, 1991; Corre et al., 1992; Curran et al., 1995).

The intermediate species in both experiments consist primarily of small olefins, in decreasing quantity as carbon number increases. The largest olefin detectable is 1-hexene — no heptene isomers are present above the detection limit of the gas chromatograph (approximately 1 – 5 ppm). Ethane is also formed early in the reaction, while polyunsaturated species such as 1,3-butadiene and ethyne are formed relatively late.

The calculated species profiles are depicted as the lines in Figures 2–4. Due to non-idealities in the mixing process, the experimental time axis is subject to some uncertainty with respect to the value used for the initial time point (Held, 1993). The time axes for the data have been shifted by the increments
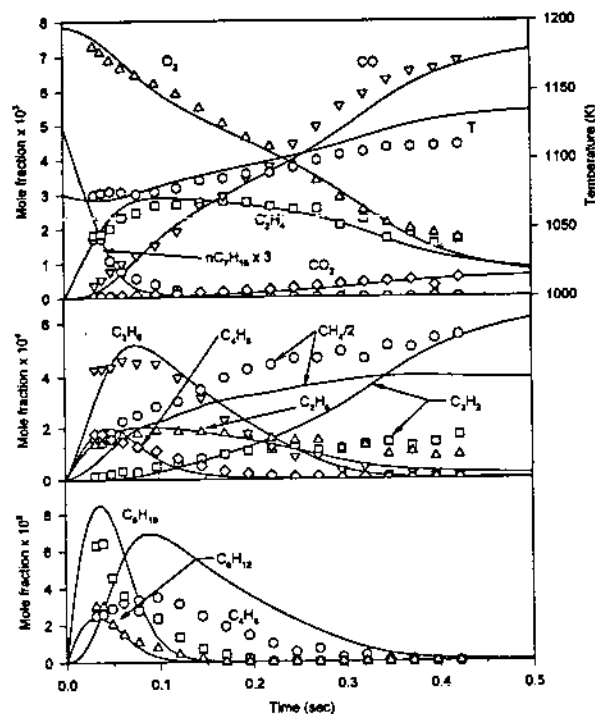
FIGURE 3   Measured (symbols) and calculated (lines) species and temperature profiles for rich
n-heptane oxidation. Data have been shifted +0.014 sec to minimize RMS difference between
calculated and measured nC_7H_{16} profiles.

consistent with experimental approximations and modeling assumptions, as
documented in the figure captions. The time increment was determined by
minimization of the weighted RMS error between the calculated and experi-
mental fuel profiles. The effects of the mixing non-idealities and the time-
shifting process have been shown elsewhere to have negligible effects upon the
remainder of the species and temperature profiles (Held, 1993).

The agreement in both cases is reasonably good, both in terms of overall
reaction rate and major intermediate distribution, with some exceptions that
are discussed below. Thermal decomposition reactions consume approxi-
mately 10% of the n-heptane in the rich oxidation case, 27% for the pyrolysis,
and a negligible amount for the lower-temperature, fuel-lean conditions. As
the sequence of conditions progresses from pyrolysis to lean oxidation, the
predominant abstractor changes from H-atom to OH radicals. Although a
minor reaction path in terms of net fuel consumption (< 5%), abstraction by
HO_2 was found have a significant effect on overall reaction rate for the
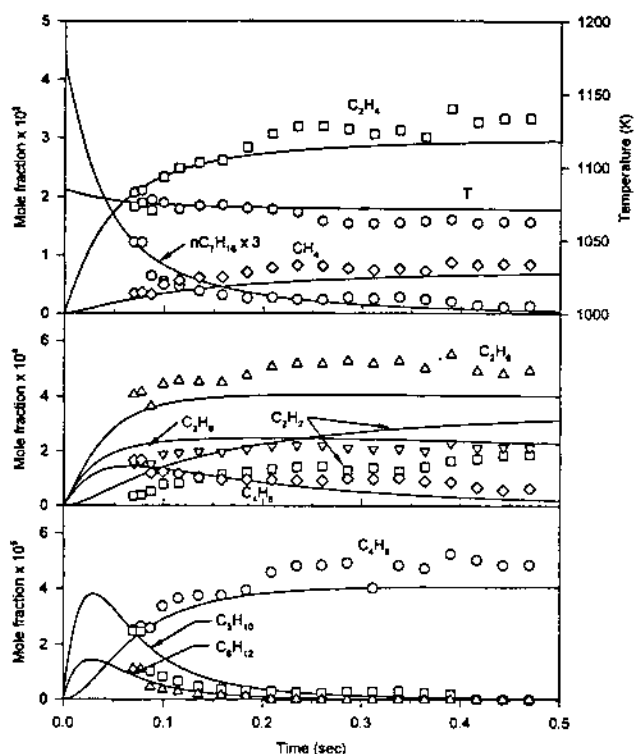
FIGURE 4 Measured (symbols) and calculated (lines) species and temperature profiles for n-heptane pyrolysis. Data have been shifted +0.050 sec to minimize RMS difference between calculated and measured nC_7H_{16} profiles.

fuel-lean conditions, due to the chain-branching thermal decomposition of the resulting hydrogen peroxide.

The formation rates of the various 1-olefins are controlled by the site-specific abstraction rate constants. Ethene is formed via numerous reaction paths, including 1-heptyl decomposition, thermal decomposition of the ethyl and 1-propyl radicals formed in 2-,3-and 4-heptyl decomposition, and further reactions of the other olefinic intermediates. The relative distribution of the larger olefins ($C_3 > C_4 > C_5 > C_6$) arises for two reasons. The reactions forming these species all result from energetically equivalent secondary C-H abstractions. The availability of only two C-H sites for 4-heptyl formation makes 1-pentene a relatively minor product. Abstraction from four C-H sites each lead to 2- and 3-heptyl radicals. However, the energetics of 3-heptyl decomposition allow for a small but significant fraction of 1-hexene formation at the expense of 1-butene.

Above 1000 K, the larger olefinic intermediates, 1-butene, pentene and hexene, react primarily by thermal decomposition to allyl and alkyl radicals, or by H-atom addition. At the fuel-lean, 940 K condition, abstraction by OH was the dominant consumption path. Sensitivity coefficients for the peak levels of the olefinic intermediates in the rich oxidation case are shown in Figure 5. As expected, the peak levels of these species are controlled by the balance between their production by the relative abstraction rates from each C-H site, and their consumption rates.

The results of sensitivity analyses for the heptane consumption and overall reaction rates in the rich oxidation case are seen in Figure 6. The fuel consumption is primarily affected by the rate constants for n-heptane thermal decomposition by C-C bond cleavage. Also, the abstraction reactions that yield the ethyl radical as an eventual product tend to increase the fuel decay rate, while those producing CH_3 inhibit the decay rate. Thermal decomposition of the C_2H_5 radical provides a significant source of H-atoms for chain branching early in the reaction, while much of the CH_3 recombines in a chain-termination process to form ethane.
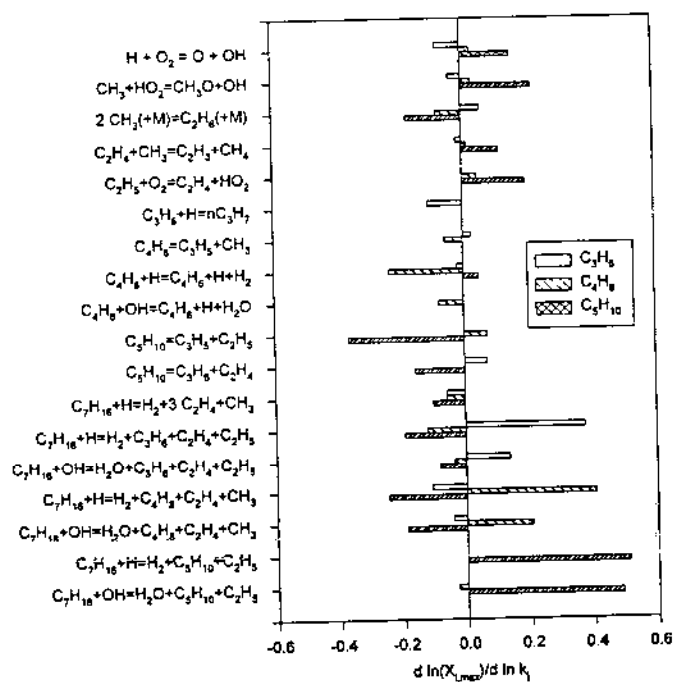
FIGURE 5 Normalized sensitivity coefficients for maximum olefin mole fractions for conditions of Figure 3.
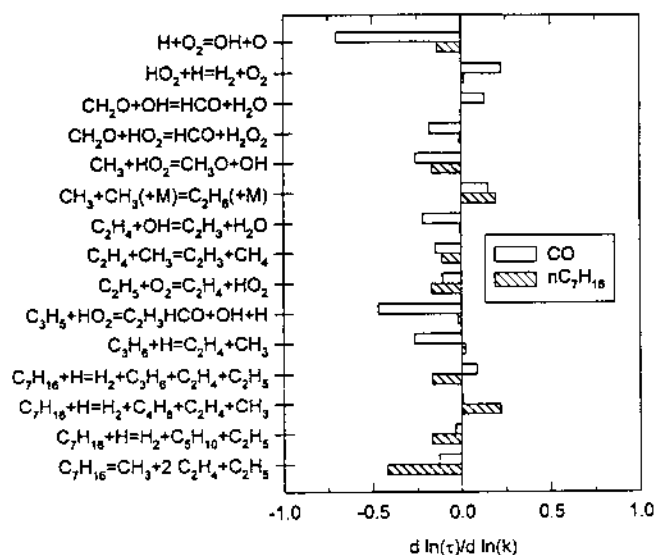
FIGURE 6 Normalized sensitivity coefficients for the time to reach 50% of maximum possible CO and 50% of n-heptane consumption for conditions of Figure 3.

Production of carbon monoxide, used as a marker of overall extent of reaction, is affected primarily by reactions involved in the $C_1 - C_3$ submechanism. The reactions consuming n-heptane are of relatively minor importance, except in that they control the distribution of olefins and small alkyl radicals, which can in turn affect the development of the labile radical pool as sources or sinks of these species. The lack of sensitivity of both the fuel-decay and CO-production rates to the large-olefin kinetics suggests that additional simplification may be possible by assuming overall reactions for their consumption.

The extreme stability of the allyl radical (C_3H_5) under these conditions permits a large accumulation of this species. Initial modeling efforts significantly overestimated the overall reaction rate under oxidation conditions. The rate constant for the reaction:

$$C_3H_5 + HO_2 \rightarrow C_2H_3 + CH_2O + OH$$
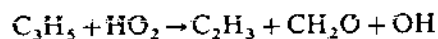
is very sensitive under these conditions, and its value is virtually unknown. For the purposes of this study, its value is used as a free parameter to fit the overall reaction rate for the rich oxidation case. The optimal value in the context of the

present mechanism is 6.72×10^{11} cc/mole/sec, approximately a factor of 15 slower than Tsang's estimate (1991).

The overprediction of 1,3-butadiene in the oxidation experiments is a cause for some concern, as this species is an important factor certain practical applications (e.g., automotive engine exhaust toxicity). The formation paths under all sets of conditions are identical — primarily from 1-olefin abstraction reaction products. Under pyrolysis conditions, little butadiene is consumed in both the experiment and computational simulation. Because the calculated formation rate in the pyrolysis case agrees well with the experiment, the discrepancy in the oxidation case is probably due to an incomplete mechanism for the butadiene oxidation. Alternatively, the excessive 1,3-butadiene levels could also be due to a decreased formation rate by the opening of other consumption routes for the C_4 and larger olefins, such as O, OH or HO_2 addition to the vinylic carbon sites.

A more precise n-heptyl scheme would also allow for rapid interconversion between the various isomers. A test case, assuming a quasi-equilibrium n-heptyl distribution, and allowing for the various decomposition paths, calculated much lower mole fractions of the larger olefinic intermediates. It is possible that some degree of isomerization could affect the intermediate distribution. Extrapolation of rate expressions for n-hexyl and s-octyl radical isomerization (Dóbé et al., 1987) to 1080 K gives values of $10^{7.1-7.2}$ sec^{-1}, comparable in magnitude to n-heptyl thermal decomposition rates at that temperature. Since the higher activation energy for thermal decomposition (29 kcal/mole vs. 11-17 kcal/mole) will reduce the role of isomerization effects at higher temperatures, isomerization is unlikely to provide important reaction paths. At the lower temperatures of the lean oxidation flow reactor and stirred reactor experiments (described below), isomerization could be expected to alter the distribution of olefinic intermediates, as evidenced by the disagreement in 1-pentene mole fractions at these conditions.

Calculations using the full Warnatz mechanism yield characteristic reaction times (excluding the induction phase) on the order of 300 sec, compared to the 0.5 second time scale of the experiments. The intermediate distribution is predominantly propene, with ethene rising late in the reaction as a secondary product of the propene oxidation and pyrolysis. The difficulty with the Warnatz mechanism cannot be corrected by simple updating of the small-molecule kinetics; substitution of the n-heptane submechanism from Warnatz for that of Table II produces a 12 second induction time for the oxidation case, followed by a reaction with a time scale of approximately 3 seconds.

STIRRED REACTOR RESULTS

Additional model validation is available through comparison to the jet-stirred reactor data of Chakir, *et al.* (1992). The data set encompasses temperatures from 900–1200 K, at a fixed pressure of one atmosphere, and residence time of 200 milliseconds. The experiments were modeled using the Chemkin Perfectly Stirred Reactor (PSR) code (Glarborg *et al.*, 1986), assuming constant pressure and temperature. The data and computational results are shown as symbols and lines, respectively, in Figures 7 and 8. The level of agreement is similar to that seen in the flow reactor calculations, with overpredictions of acetylene and 1-pentene. Reaction path analysis indicates results essentially similar to those found for the flow reactor conditions.

The formation rate of CO is underpredicted for the fuel-rich case, and the oxidation rate of CO at 1050 K is underpredicted for the fuel-lean conditions. The former is possibly due to remaining uncertainties in the C_2H_4 oxidation mechanism, particularly with regard to the rate constants and reaction channels for $C_2H_3 + O_2$ (Westmoreland, 1992; Bozzelli and Dean, 1993;
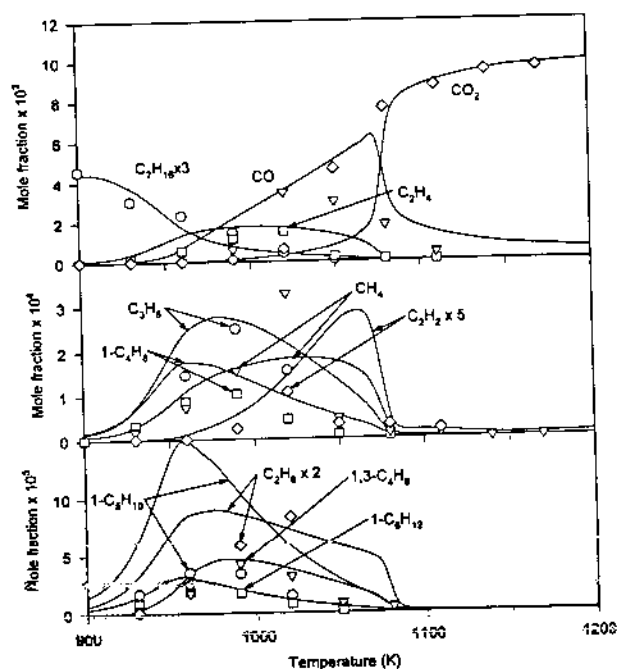
FIGURE 7 Measured (symbols) and calculated (lines) species profiles for *n*-heptane stirred reactor oxidation. Inlet conditions are $p = 1$ atm, $X_{nC_7H_{16}} = 0.0015$, $\phi = 0.5$, $\tau = 0.20$ sec.
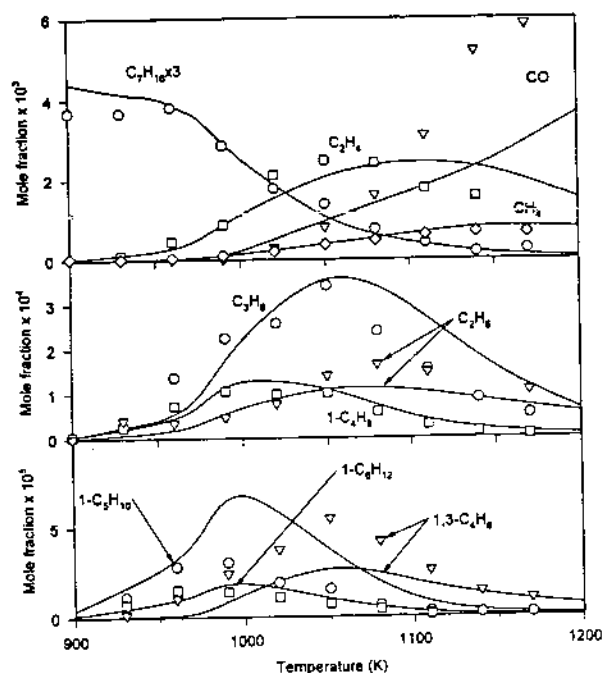
FIGURE 8   Measured (symbols) and calculated (lines) species profiles for n-heptane stirred reactor oxidation. Inlet conditions are $p = 1$ atm, $X_{nC_7H_{16}}$, $i = 0.0015$, $\phi = 2.0$, $\tau = 0.20$ sec.

Marinov et al., 1995; Marinov and Malte, 1995; Westmoreland, 1996). The latter may possibly be due to experimental difficulties maintaining constant temperature conditions in the stirred reactor under the high energy release rate associated with CO oxidation.

SHOCK TUBE RESULTS

While flow and stirred reactor results provide a large amount of information regarding species distributions and overall reaction rates, the accessible range of initial temperatures is limited to less than approximately 1200 K. To extend the validation range of the mechanism, the data of Vermeer et al. (1972) are used as a test of the higher temperature kinetics. A single parameter, ignition delay as measured by pressure rise, is used as the basis for comparison. The initial composition is fixed at 2.5% n-hyptane, 27.5% oxygen (stoichiometric equivalence ratio) and balance argon. The initial pressure is varied from approximately 1.5 to 3.5 atmospheres, and the initial temperature from 1270 to 1580 K.

A constant volume, zero dimensional model is used to simulate these experiments. The induction time is defined as the extrapolation of the maximum temporal derivative of pressure back to the initial pressure.

A comparison of the calculated induction time parameters is shown in Figure 9, along with the data of Vermeer et al. (1972). The overall agreement is generally satisfactory, within the limitations of the experimental technique and the computed inaccuracy due to the constant volume assumption.

The consumption path for n-heptane is H-atom abstraction throughout the range of conditions studied. At the highest temperatures, thermal decomposition consumes approximately one third of the fuel. The rate-controlling steps are primarily the small-molecule reactions, as indicated by the sensitivity analysis in Figure 10. Steps involving the production and consumption of H-atoms are particularly important due to the branching reaction $H + O_2 \rightarrow OH + O$. The ignition delay is generally less sensitive to rate constants of reactions involving n-heptane, although at higher temperatures, the thermal decomposition rate constant begins to become important.

PREMIXED FLAME SPEED RESULTS

Data for the premixed laminar flame speed of n-heptane are relatively few. The two data sets chosen for inclusion in this comparison are the only data for an
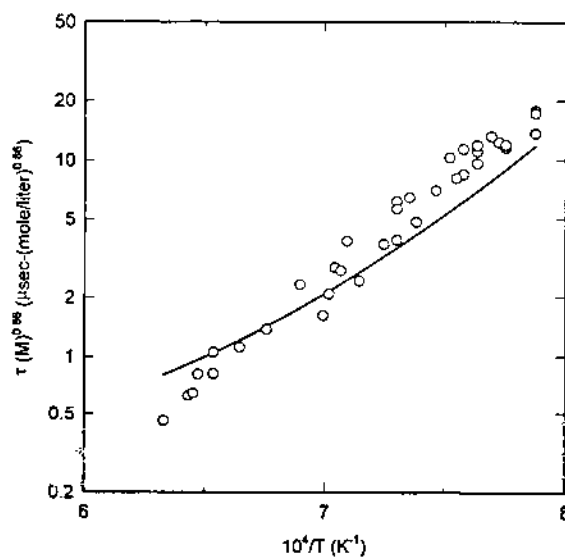
FIGURE 9 Shock tube ignition delay. Symbols are data of Vermeer et al. (1972), lines are calculated values with mechanism of Table II.
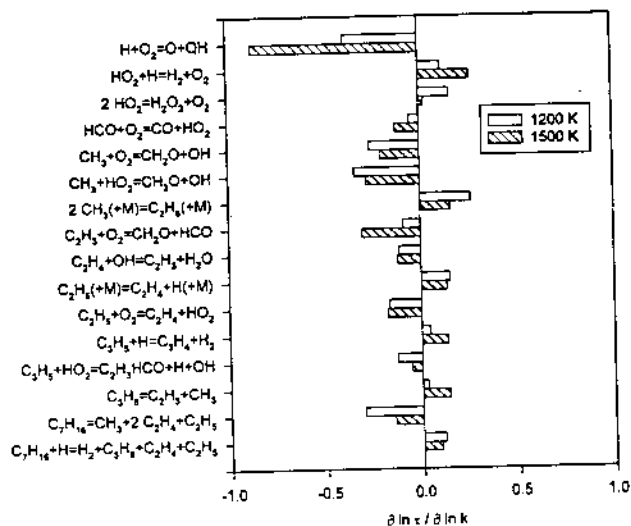
FIGURE 10   Normalized sensitivity coefficients for shock tube ignition delay, $p = 2.5$ atmospheres, constant volume simulation.

initial temperature of 298 K, and are the same two sets used in the work of Warnatz (1984a). Gerstein et al. (1951) used the flame propagation rate and surface area in a horizontal tube to measure the overall burning rate, while Gibbs and Calcote (1959) used a Bunsen flame method. Both methods are subject to considerable uncertainty with regard to secondary effects, such as flame stretch (Law, 1988) and heat loss to tube walls.

The calculated flame speeds with the present mechanism are shown in Figure 11, along with the aforementioned data sets, and the calculated flame speeds reported by Warnatz (1984a). Definitive conclusions regarding the relative performance of the mechanism are difficult to draw, due to the quantitative and qualitative disagreement between the data sets. It is sufficient to note that the calculated speeds are in reasonable agreement with the data of Gibbs and Calcote, although the disagreement is fairly large at lean equivalence ratios.

The dominant fuel consumption paths vary somewhat as a function of equivalence ratio. Abstraction by H and OH is still the predominant reaction path, although at higher equivalence ratios, thermal decomposition of the fuel becomes increasingly important. Superposition of the fuel and temperature profiles under all calculated conditions indicates over 99% consumption of the n-heptane before the local temperature has reached 1500 K. Essentially, the thermal instability of the fuel, combined with the characteristic residence time
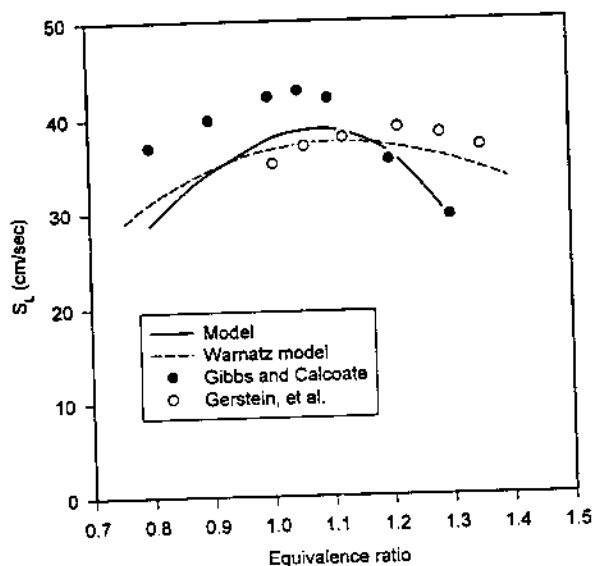
FIGURE 11   Premixed laminar flame speed as a function of equivalence ratio, *n*-heptane/air flames, initial temperature = 298 K.

in the flame preheat zone, limits the temperature at which the fuel can survive to approximately 1500 K at one atmosphere.

The sensitivity coefficients for laminar flame speed are shown in Figure 12. Interestingly, the flame speed is almost totally insensitive to the rate constants for the fuel-consuming reactions. The main rate-controlling steps are the $H + O_2 \rightarrow OH + O$ branching reaction over the full range of conditions, and CO oxidation $(CO + OH \rightarrow CO_2 + H)$ at lean to slightly rich equivalence ratios.

The primary means by which hydrocarbon chemistry affects calculated flame speeds is through the formation and destruction of H-atoms through the reactions of C_3H_5, C_2H_3 and CH_3:

$$C_3H_5 + H = C_3H_4 + H_2$$

$$C_2H_3(+M) = C_2H_2 + H(+M)$$

$$CH_3 + CH_3 = C_2H_5 + H$$
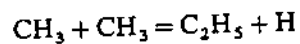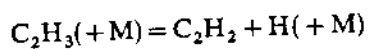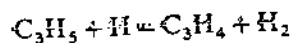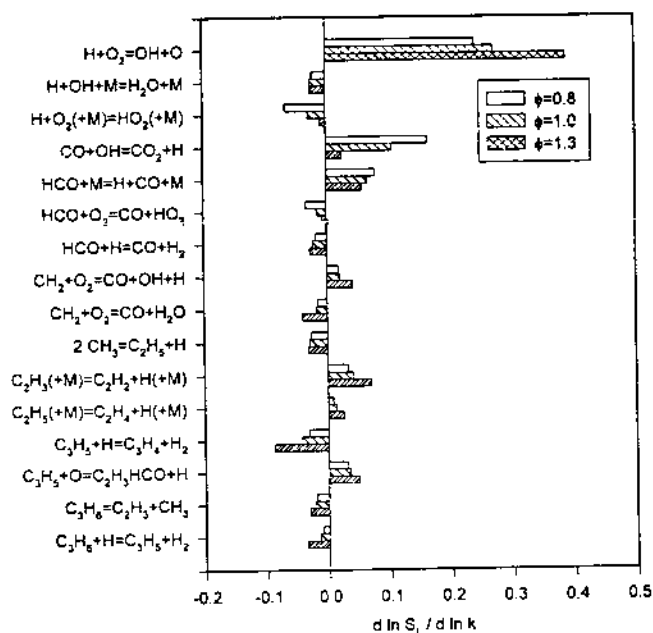
FIGURE 12   Normalized sensitivity coefficients for laminar flame speed.

The allyl radical (C_3H_5) is intially formed mainly by allylic H-atom abstraction from propene. Because of its high resonant stability, thermal decomposition is a minor consumption path for allyl — in fact, the reverse reaction forms part of an important catalytic chain removal of hydrogen atoms from the system:

$$C_3H_5 + H = C_3H_4 + H_2$$

$$C_3H_4 + H = C_3H_5$$
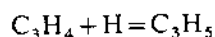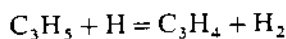
The competing reaction with oxygen atoms,

$$C_3H_5 + O = C_2H_3HCO + H$$
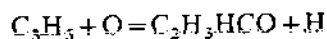
provides an alternative, chain-propagating step, and the primary means of allyl destruction under flame conditions. Although radical–radical reactions involving allyl are of great importance for these flame calculations, few experimental rate constant data presently exist. Clearly, this area of the

mechanism requires additional study and development, and certain conclusions drawn may be influenced by uncertainties in the submechanisms.

CONCLUSIONS

A new, semi-empirical *n*-heptane model reproduces overall reaction rate and intermediate species distributions measured in flow reactor experiments. The treatment of site-specific abstraction reactions, and individual alkyl radical decomposition paths permits substantial increase in the level of detail in the model without significantly increasing the number of species required. Further reduction could be achieved by assuming rapid thermal decomposition of the larger olefinic intermediates.

The important overall rate-determining processes generally involve the small-molecule and radical chemistry, such as $H + O_2$ branching and CO oxidation. The main participation of the hydrocarbon chemistry is as sources or sinks of H-atoms. The allyl radical is particularly important to overall reaction rates because of its ability to build up in large concentrations as a result of its resonant stability. The details of the propene submechanism still require further development, especially the allyl + radical reactions.

Clearly, the level of detail that needs to be retained in such a semi-empirical model is governed by the intended use of the mechanism. Premixed laminar flame speeds are an example of a situation where large-olefin formation could be neglected without seriously affecting the calculated results. For situations where intermediate species formation is important, such as in hydrocarbon emissions formation chemistry, considerably more detail must be retained.

While the present work has focused upon *n*-heptane as an intial fuel, the techniques used can be extended to other linear alkanes with little modification. The only additional species required, aside from the fuel itself, would be any unique 1-olefins formed via β-scission of the fuel's alkyl radicals. In the present work, the olefins react increasingly via thermal decomposition as their carbon number increases. Therefore even these species could conceivably be eliminated from the mechanism by treating their decomposition as instantaneous.

Further work is required for modeling of branched alkanes, such as iso-octane (2, 2, 4-trimethyl pentane). These species also form branched olefins, such as isobutene (2-methyl propene), which can have significant effects on the radical pool due to the high resonant stability of their allylic radicals. Work is presently underway to expand this section of the mechanism. Complex

mixtures of alkanes can also be simulated at minimal additional computational expense, since most of the alkyl radical decomposition products will be duplicated.

Acknowledgements

References

Atri, G. M., Baldwin, R. R., Jackson, K. and Walker, R. W. (1977) The reaction of OH radicals and HO$_2$ radicals with carbon monoxide. *Combust. Flame*, **30**, 1.

Axelsson, E. I., Brezinsky, K., Dryer, F.L., Pitz, W. J. and Westbrook, C. K. (1986) Chemical kinetic modeling of the oxidation of large alkane fuels: *n*-Octane and iso-octane. *Twenty-first Symp. (Intl.) on Combustion*, p. 783.

Baldwin, R. R., Fuller, A. R., Longthorn, D. and Walker, R. W. (1974) Oxidation of formaldehyde in KCl-coated vessels. *J. Chem. Soc. Faraday I*, **70**, 1257.

Baulch, D. L., Drysdale, D. D., Horne, D. E. and Lloyd, A. C. (1972) Homogeneous gas phase reactions of the H$_2$-O$_2$ system. In *Evaluated kinetic data for high temperature reactions*. London: Butterworths.

Baulch, D. L., Drysdale, D. D., Duxbury, J. and Grant, S. J. (1976) Homogeneous gas phase reaction of the O$_2$-O$_3$ system, the CO-O$_2$-H$_2$ systems and of sulphur-containing species. In *Evaluated kinetic data for high temperature reactions*, London: Butterworths.

Baulch, D. L., Cox, R. A., Hampson, R. F., Kerr, J. A., Troe, J. and Watson, R. T. (1980) *J. Phys. Chem. Ref. Data*, **9**, 295.

Bowman, C. T., Hanson, R. K. and Davidson, D. F. et al. (1996) *GRI-MECH, Version 2.11.* http://www.me.berkeley.edu/gri_mech/

Bozzelli, J. W. and Dean, A. M. (1993) Hydrocarbon radical reactions with O$_2$: Comparisons of allyl, formyl and vinyl to ethyl. *J. Phys. Chem.*, **97**, 4427.

Brouwer, L., Cobos, C. J., Troe, J., Dubai, J.-R. and Crimm, F. F. (1987) Specific rate constants $k_{E,j}$ and product state distributions in simple bond fission reactions. II. Application to HOOH→OH + OH. *J. Chem. Phys.*, **86**, 6171.

Bui-Pham, M. and Seshadri, K. (1991) Comparisons between experimental measurements and numerical calculations of the structure of heptane-air diffusion flames. *Combust. Sci. and Tech.*, **79**, 293.

Card, J. M. and Williams, F. A. (1992) Asymptotic analysis of the structure and extinction of spherically symmetrical *n*-heptane diffusion flames. *Combust. Sci. and Tech.*, **84**, 91.

Card, J. M. and Williams, F. A. (1993) Asymptotic analysis for the burning of *n*-heptane droplets using a four-step reduced mechanism. *Combust. Flame*, **93**, 375.

Chakir, A., Bellimam, M., Boettner, J. C. and Cathonnet, M. (1992) Kinetic study of *n*-heptane oxidation. *Int. J. Chem. Kinet.*, **24**, 385.

Clark, J. C. and Dove, J. E. (1973) Examination of possible non-Arrhenius behavior in reactions. *Can. J. Chem.*, **51**, 2147.

Cobos, C. J., Hippler, H. and Troe, J. (1985) High-pressure falloff curves and specific rate constants for the reactions $H + O_2 \rightleftharpoons HO_2 \rightleftharpoons HO + O$. *J. Phys. Chem.*, **89**, 342.

Cohen, N. (1991) Are reaction rate coefficients additive? Revised transition state theory calculations for $OH + $ alkane reactions. *Int. J. Chem. Kinet.*, **23**, 397.

Cohen, N. and Westberg, K. R. (1983) Chemical kinetic data sheets for high-temperature chemical reactions. *J. Phys. Chem. Ref. Data*, **12**, 531.

Cohen, N. and Westberg, K. R. (1986) The use of transition-state theory to extrapolate rate coefficients for reactions of O-atoms with alkanes. *Int. J. Chem. Kinet.*, **18**, 99.

Colket, M. B., Naegeli, D. W. and Glassman, I. (1975) High-temperature pyrolysis of acetaldehyde. *Int. J. Chem. Kinet.*, **7**, 223.

Colket, M. B., III, Naegeli, D. W. and Glassman, I. (1977) High-temperature oxidation of acetaldehyde. *Sixteenth Symp. (Intl.) on Combustion*, p. 1023.

Corre, C., Dryer, F. L., Pitz, W. J. and Westbrook, C. K. (1992) Two-stage *n*-butane flame: A comparison between experimental measurements and modeling results. *Twenty-fourth Symp. (Intl.) on Combustion*.

Curran, H. J., Gaffuri, P. and Pitz, W. J. et al. (1995) *A modelling study of the combustion of n-heptane and iso-octane in a high pressure turbulent flow reactor*. Presented at the Central States/Western States/ Mexican National Sections Meeting, The Combustion Institute, San Antonio, TX.

Dagaut, P., Cathonnet, M. and Boettner, J. C. (1990) Propyne oxidation: A modeling study. *Combust. Sci. and Tech.*, **71**, 111.

Dagaut, P., Cathonnet, M. and Boettner, J. C. (1991) Kinetics of ethane oxidation. *Int. J. Chem. Kinet.*, **23**, 437.

Dagaut, P., Cathonnet, M. and Boettner, J.-C. (1992) A kinetic modeling study of propene oxidation in JSR and flame. *Combust. Sci. and Tech.*, **83**, 167.

Dean, A. M. (1985) Predictions of pressure and temperature effects upon radical addition and recombination reactions. *J. Phys. Chem.*, **89**, 4600.

Dóbé, S., Bérces, T., Réti, F. and Márta, F. (1987) Isomerization of *n*-hexyl and *s*-octyl radicals by 1, 5 and 1, 4 intramolecular hydrogen atom transfer reactions. *Int. J. Chem. Kinet.*, **19**, 895.

Dryer, F. L. (1991) The phenomenology of modeling combustion chemistry. In Bartok, W. and Sarofim, A. F. (Eds), *Fossil fuel combustion: A sourcebook*, Wiley.

Egolfopoulos, F. N., Du, D. X. and Law, C. K. (1992) A comprehensive study of methanol kinetics in freely-propagating and burner-stabilized flames, flow and static reactors, and shock tubes. *Combust. Sci and Tech.*, **83**, 33.

Felder, W. and Madronich, S. (1986) High temperature photochemistry (HTP): Kinetics and mechanism studies of elementary combustion reactions over 300–1700 K. *Combust. Sci. and Tech.*, **50**, 135.

Gerstein, M., Levine, O. and Wong, E. L. (1951) Flame propagation. II. The determination of fundamental burning velocities of hydrocarbons by a revised tube method. *Ind. Eng. Chem.*, **73**, 418.

Gibbs, G. J. and Calcote, H. F. (1959) Effect of molecular structure on burning velocity. *J. Chem. Eng. Data*, **4**, 226.

Glarborg, P., Kee, R. J., Grcar, J. F. and Miller, J. A. (1986) *PSR: A Fortran program for modeling well-stirred reactors*. SAND86-8209, Sandia National Laboratories, Livermore, CA.

Hampson, R. F. (1980) *Chemical kinetic and photochemical data sheets for atmospheric reactions*. FAA-EE-80-17, U.S. Dept. of Transportation, FAA, Washington, DC.

Heinemann, P., Hoffman-Sievert, R. and Hoyermann, K. (1986) Direct study of the reactions of vinyl radicals with hydrogen and oxygen atoms. *Twenty-first Symp. (Intl.) on Combustion*, p. 865.

Held, T. J., Dryer, F. L., Brezinsky, K., Pitz, W. J. and Westbrook, C. K. (1988) *The high temperature oxidation of isobutene*. Presented at the Eastern States Section Meeting, The Combustion Institute, Clearwater, FL.

Held, T. J. (1993) The oxidation of methanol, isobutene and methyl tertiary-butyl ether. Ph.D. dissertation, Princeton University.

Held, T. J., and Dryer, F. L. (1994) An experimental and computational study of methanol oxidation in the intermediate and high temperature regimes. Twenty-fifth Symp. (Intl.) on Combustion, p. 901.

Held, T. J. and Dryer, F. L. (1996) Unpublished work.

Hippler, H., Troe, J. and Willner, J. (1990) Shock wave study of the reaction $HO_2 + HO_2 \rightarrow H_2O_2 + O_2$: Confirmation of a rate constant minimum near 700 K. J. Chem. Phys., 93, 1755.

Hippler, H. and Troe, J. (1992) Rate constants of the reaction $HO + H_2O_2 \rightarrow HO_2 + H_2O$ at $T \geqslant$ 1000 K. Chem. Phys. Lett., 192, 333.

Hochgreb, S. and Dryer, F. L. (1992) A comprehensive study on CH_2O oxidation kinetics. Combust. Flame, 91, 257.

Hoyermann, K., Loftfield, N. S., Sievert, R. and Wagner, H. G. (1981) Mechanisms and rates of the reactions of CH_3O and CH_2OH radicals with H-atoms. Eighteenth Symp. (Intl.) on Combustion, p. 831.

Jachimowski, C. J. (1977) An experimental and analytical study of acetylene and ethylene oxidation behind shock waves. Combust. Flame, 29, 55.

Jackson, G. S. and Avedesian, C. T. (1993) Presented at the Eastern States Section Meeting, The Combustion Institute, Princeton, NJ.

Kaiser, E. W., Westbrook, C. K. and Pitz, W. J. (1986) Acetaldehyde oxidation in the negative temperature regime: Experimental and modeling results. Int. J. Chem. Kinet., 18, 655.

Kee, R. J., Grear, J. F., Smooke, M. D. and Miller, J. A. (1985) A Fortran program for modeling steady laminar one-dimensional premixed flames. SAND85-8240, Sandia National Laboratories, Livermore, CA.

Kee, R. J., Rupley, F. M. and Miller, J. A. (1989) Chemkin-II: A Fortran chemical kinetics package for the analysis of gas-phase chemical kinetics. SAND89-8009, Sandia National Laboratories, Livermore, CA.

Kennedy, S. P., Brezinsky, K. and Dryer, F. L. (1985) Presented at the Eastern States Section Meeting, The Combustion Institute, Philadelphia, PA.

Kent, J. H. and Williams, F. A. (1974) Extinction of laminar diffusion flames for liquid fuels. Fifteenth Symp. (Intl.) on Combustion, p. 315.

Kern, R. D., Singh, H. J. and Wu, C. H. (1988) Thermal decomposition of 1,2-butadiene. Int. J. Chem. Kinet., 20, 731.

Kiefer, J. H., Wei, H. C., Kern, R. D. and Wu, C. H. (1985) The high temperature pyrolysis of 1,3-butadiene: Heat of formation and rate of dissociation of vinyl radical. Int. J. Chem. Kinet., 17, 225.

Kim, T. J., Yetter, R. A. and Dryer, F. L. (1994) New results on moist CO oxidation: High pressure, high temperature experiments and comprehensive kinetic modeling. Twenty-fifth Symp. (Intl.) on Combustion, p. 759.

Law, C. K. (1988) Dynamics of stretched flames. Twenty-second Symp. (Intl.) on Combustion, p.1381.

Lin, M. T. and Laidler, K. J. (1968) Can. J. Chem., 46, 479.

Lindstedt, R. P. and Maurice, L. Q. (1995) Detailed kinetic modelling of n-heptane combustion. Combust. Sci. and Tech., 107, 317.

Lissi, E. A., Massiff, G. and Villa, A. E. (1973) Oxidation of carbon monoxide by methoxy-radicals. J. Chem. Soc. Faraday. I, 69, 346.

Liu, A., Mulac, W. A. and Jonah, C. D. (1988) Rate constants for the gas-phase reactions of OH radicals with 1,3-butadiene and allene at 1 atm and over the temperature range 305–1173 K. J. Phys. Chem., 92, 131.

Lutz, A. E., Kee, R. J. and Miller, J. A. (1987) SENKIN: A Fortran program for predicting homogeneous gas phase chemical kinetics with sensitivity analysis. SAND87-8248, Sandia National Laboratories, Livermore, CA.

Marchese, A. J., Choi, M. Y. and Dryer, F. L. (1994) MAE Report No.1999, Department of Mechanical and Aerospace Engineering, Princeton University, Princeton NJ.

Marchese, A. J., Dryer, F. L. and Held, T. J. (1995) Transient numerical modeling of the combustion of bi-component liquid droplets: Heptane/hexadecane mixtures. Presented at the Central

States/Western States/Mexican National Sections Meeting, The Combustion Institute, San Antonio, TX.

Marinov, N. M., Pitz, W. J. and Westbrook, C. K. (1995) *Numerical study of ethylene and acetylene laminar flame speeds.* Paper No. 95S-029. Presented at the Central States/Western States/Mexican National Sections Meeting, The Combustion Institute, San Antonio, TX. p. 151.

Marinov, N. M. and Malte, P. C. (1995) Ethylene oxidation in a well-stirred reactor. *Int. J. Chem. Kinet.*, **27**, 957.

Michael, J. V. and Sutherland, J. W. (1988) Rate constant for the reaction of H with H_2O and OH with H_2 by the flash photolysis-shock tube technique over the temperature range 1246–2297 K. *J. Phys. Chem.*, **92**, 3853.

Michael, J. V. and Wagner, A. F. (1990) Rate constants for the reactions $O + C_2H_2$ and $O + C_2D_2 \rightarrow$ products, over the temperature range ~850–1950 K, by the flash photolysis-shock tube technique. Determination of the branching ratio and a further theoretical analysis. *Ber. Bunsenges. Phys. Chem.*, **94**, 2453.

Miller, J. A., Mitchell, R. E., Smooke, M. D. and Kee, R. J. (1982) Toward a comprehensive chemical kinetic mechanism for the oxidation of acetylene: Comparisons of model predictons with results from flame and shock tube experiments. *Nineteenth Symp. (Intl.) on Combustion*, p. 181.

Miller, J. A. and Bowman, C. T. (1989) Mechanism and modeling of nitrogen chemistry in combustion. *Prog. Energy Combust. Sci.*, **15**, 287.

Miller, J. A. and Melius, C. F. (1988) A theoretical analysis of the reaction between hydroxyl and acetylene. *Twenty-second Symp. (Intl.) on Combustion*, p. 1031.

NASA (1985) *Chemical kinetics and photochemical data for use in stratospheric modeling.* JPL Publ. 85–37, NASA Panel for Data Evaluation.

Page, M., Lin, M. C., He, Y. and Choudhury, T. K. (1989) Kinetics of the methoxy radical decomposition reaction: Theory and experiment. *J. Phys. Chem.*, **93**, 4404.

Pirraglia, A. N., Michael, J. V., Sutherland, J. W. and Klemn, R. B. (1989) A flash photolysis-shock tube kinetic study of the H-atom reaction with O_2: $H + O_2 \Leftrightarrow OH + O$ (962 K $\leqslant T \leqslant$ 1705 K) and $H + O_2 + Ar \rightarrow HO_2 + Ar$ (746 K $\leqslant T \leqslant$ 987 K) *J. Phys. Chem.*, **93**, 282.

Rao, V. S., Takeda, K. and Skinner, G. B. (1988) Formation of H and D atoms in pyrolysis of 1,3-butadiene and 1, 3-butadiene-1, 1, 4, 4, -d4 behind shock waves. *Int. J. Chem. Kinet.*, **20**, 153.

Reid, I. A. B., Robinson, C. and Smith, D. B. (1988) Spontaneous ignition of methane: Measurement and kinetic model. *Twenty-second Symp. (Intl.) on Combustion*, p. 1833.

Roth, P. and Just, T. (1984) Kinetics of the high temperature, low concentration CH_4 oxidation verified by H and O atom measurements. *Twentieth Symp. (Intl.) on Combustion*, p. 807.

Schatz, G. C., Wagner, A. F. and Dunning Jr., T. H. (1984) A theoretical study of deuterium isotope effects in the reactions $H_2 + CH_3$ and $H + CH_4$ *J. Phys. Chem.*, **88**, 221.

Slack, M. W (1977) Rate coefficient for $H + O_2 + M = HO_2 + M$ evaluated from shock tube measurements of induction times. *Combust. Flame*, **28**, 241.

Slagle, I. R. Ratajczak, E. and Gutman, D. (1986) Study of the thermochemistry of the $C_2H_5 + O_2 \Leftrightarrow C_2H_5O_2$ and $t\text{-}C_4H_9 + O_2 \Leftrightarrow t\text{-}C_4H_9O_2$ reactions and of the trend in the alkylperoxy bond strengths. *J. Phys. Chem.*, **90**, 402.

Slagle, I. R. Sarzynski, D. and Gutman, D. (1987) Kinetics of the reaction between methyl radicals and oxygen atoms between 294 and 900 K. *J. Phys. Chem.*, **91**, 4375.

Slagle, I. R. and Gutman, D. (1986) Kinetics of the reaction of C_3H_3 with molecular oxygen from 293–900 K. *Twenty-first Symp. (Intl.) on Combustion*, p. 875.

Sutherland, J. W., Michael, J. V. and Klemm, R. B. (1986a) Rate constant for the $O(^3P) + CH_4 \rightarrow OH + CH_3$ reaction obtained by the flash photolysis-shock tube technique over the temperature range 763 $\leqslant T \leqslant$ 1755 K. *J. Phys. Chem.*, **90**, 5941.

Sutherland, J. W., Michael, J. V., Pirraglia, A. N., Nesbitt, F. L. and Klemm, R. B. (1986b). Rate constant for the reaction of $O(^3P)$ with H_2 by the flash photolysis-shock tube and flash photolysis-resonance fluorescence techniques; 504 K $\leqslant T \leqslant$ 2495 K. *Twenty-first Symp. (Intl.) on Combustion*, p. 929.

Sutherland, J. W., Patterson, P. M. and Klemm, R. B. (1990) Rate constants for the reaction $O(^3P) + H_2O = OH + OH$, over the temperature range of 1053–2033 K using 2 different techniques. *Twenty-third Symp. (Intl.) on Combustion*, p. 51.

Timonen, R. S., Ratajczak, E. and Gutman, D. (1987a) Kinetics of the reaction between formyl radicals and atomic hydrogen. *J. Phys. Chem.*, 91., 692.

Timonen, R. S., Ratajczak, E., Gutman, D. and Wagner, A. F. (1987b) The addition and dissociation reaction $H + CO \rightleftharpoons HCO$. 2. Experimental studies and comparison with theory. *J. Phys. Chem.*, 91, 5325.

Timonen, R. S., Ratajczak, E. and Gutman, D. (1988) Kinetics of the reactions of the formyl radical with oxygen, nitrogen dioxide, chlorine and bromine. *J. Phys. Chem.*, 92, 651.

Tsang, W. (1978a) Thermal stability of cyclohexane and 1-hexene. *Int. J. Chem. Kinet.*, 10, 1119.

Tsang, W. (1978b) Thermal decomposition of cyclopentane and related compounds. *Int. J. Chem. Kinet.*, 10, 599.

Tsang, W. (1988) Chemical kinetic data base for combustion chemistry. Part 3. Propane. *J. Phys. Chem. Ref. Data*, 17, 887.

Tsang, W. (1989) Rate constants for the decomposition and formation of simple alkanes over extended temperature and pressure ranges. *Combust. Flame*, 78, 71.

Tsang, W. (1991) Chemical kinetic data base for combustion chemistry. Part 5. Propene. *J. Phys. Chem. Ref. Data*, 20, 221.

Tsang, W. and Hampson, R. F. (1986) Chemical kinetic data base for combustion chemistry. Part I. Methane and related compounds. *J. Phys. Chem. Ref. Data*, 15, 1087.

Tsang, W. and Walker, J. A. (1992) Pyrolysis of 1,7-octadiene and the kinetic and thermodynamic stability of allyl and 4-pentenyl radicals. *J. Phys. Chem.*, 96, 8378.

Tully, F. P., Droege, A. T., Koszykowski, M. L. and Melius, C. F. (1986) Hydrogen-atom abstraction from alkanes by OH. 2. Ethane. *J. Phys. Chem.*, 90, 691.

Tully, F. P. (1988) Hydrogen atom abstraction from alkenes by OH. Ethene and 1-butene. *Chem. Phys. Lett.*, 143, 510.

Vermeer, D. J., Meyer, J. W. and Oppenheim, A. K. (1972) Auto-ignition of hydrocarbons behind reflected shock waves. *Combust. Flame*, 18, 327.

Wagner, A. F., and Wardlaw, D. M. (1988) Study of the recombination reaction $CH_3 + CH_3 \rightarrow C_2H_6$. 2. Theory. *J. Phys. Chem.*, 92, 2462.

Walker, R. W. (1975) A critical survey of rate constants for reactions in gas-phase hydrocarbon oxidation, Burlington House.

Walker, R. W. (1977) Rate constants for reaction in gas-phase hydrocarbon oxidation. In *Gas Kinetics and Energy Transfer: A Specialist Periodical Report*, The Chemical Society, Chap. 7.

Wantuck, P. J., Oldenborg, R. C., Baughcum, S. L. and Winn, K. R. (1987) Removal rate constant measurements for CH_3O by O_2 over the 298–973 K range. *J. Phys. Chem.*, 91, 4653.

Warnatz, J. (1981) The structure of laminar alkane-, alkene-, and acetylene flames. *Eighteenth Symp. (Intl.) on Combustion*, p. 369.

Warnatz, J. (1984a) Chemistry of high-temperature combustion of alkanes up to octane. *Twentieth Symp. (Intl.) on Combustion*, p. 845.

Warnatz, J. (1984b) In Gardiner, W.C., Jr. (Ed.), *Combustion chemistry*, Springer-Verlag, Chap.5.

Weissman, M. A. and Benson, S. W. (1988) Rate parameters for the reactions of C_2H_3 and C_4H_5 with H_2 and C_2H_2. *J. Phys. Chem.*, 92, 4080.

Westbrook, C. K. and Dryer, F. L. (1984) Chemical kinetic modeling of hydrocarbon combustion. *Prog. Energy Combust. Sci.*, 10, 1.

Westbrook, C. K. and Pitz, W. J. (1984) A comprehensive chemical kinetic reaction mechanism for oxidation and pyrolysis of propane and propene. *Combust. Sci. and Tech.*, 37, 117.

Westbrook, C. K. and Pitz, W. J. (1993) A chemical kinetic mechanism for the oxidation of paraffinic hydrocarbons needed for primary reference fuels. Presented at the Western States Section Meeting, The Combustion Institute, Salt Lake City, UT.

Westmoreland, P. R. (1992) Thermochemistry and kinetics of $C_2H_3 + O_2$ reactions. *Combust. Sci. and Tech.*, 82, 151.

Westmoreland, P. R. (1996) Personal communication.

Wu, C. H. and Kern, R. D. (1987) Shock tube study of allene pyrolysis. *J. Phys. Chem.*, 91, 6291.

Yetter, R. A., Dryer, F. L. and Rabitz, H. (1991) A comprehensive reaction mechanism for carbon monoxide/hydrogen/oxygen kinetics. *Combust. Sci and Tech.*, 79, 97.